

A paleoenvironmental reconstruction of Laguna Babícora, Chihuahua, Mexico based on ostracode paleoecology and trace element shell chemistry

Manuel R. Palacios-Fest¹, Ana Luisa Carreño², José R. Ortega-Ramírez³ & Guillermo Alvarado-Valdéz⁴

¹Terra Nostra Earth Sciences Research, 3220 West Ina Road #8105, Tucson, AZ 85741, USA

(E-mail: terra_nostra_mx@yahoo.com.mx)

²Instituto de Geología, UNAM, Circuito Exterior, C.U., Delegación de Coyoacán, 04510 D.F., Mexico

(E-mail: anacar@servidor.unam.mx)

³Instituto de Geofísica, UNAM, Circuito Exterior, C.U., Delegación de Coyoacán, 04510 D.F., Mexico

(E-mail: jortega@tonatiuh.igeofcu.unam.mx)

⁴Departamento de Geología, Universidad de San Luis Potosí, 78290 San Luis Potosí, SLP, Mexico

(E-mail: alvarado@deimos.tc.uaslp.mx)

Received 15 February 2001; accepted 3 April 2001

Key words: ostracodes, paleotemperature, lake evolution, Pleistocene-Holocene

Abstract

Paleoecology of Laguna Babícora, Chihuahua, Mexico was reconstructed using ostracode faunal assemblages and shell chemistry. The paleolimnological record is used to show the magnitude of paleoclimatic changes in the area from 25,000 years to the present.

Faunal assemblages consist of four species of the genus *Limnocythere*: *L. sappaensis*, *L. ceriotuberosa*, *L. bradburyi* and *L. platyforma*, all associated with *Candona caudata*, *Candona patzcuaro* and *Cypridopsis vidua*. A paleosalinity index developed from these assemblages indicates that the lake's salinity fluctuated frequently from oligo- to meso-haline conditions during the last ~ 25,000 years. This pattern and low salinity range are in good agreement with modern TDS (here used as an indicator of salinity) values recorded from 26 wells and one spring from the area (258–975 mg l⁻¹). To estimate paleotemperature we examined the trace element content (Mg/Ca ratios) from individual valves of *L. ceriotuberosa* and *L. platyforma*, the two species most commonly recorded in Laguna Babícora.

Shell Mg/Ca ratios of 204 specimens of these two species were used to estimate water temperature (Mg/Ca) by means of experimental standard coefficients. Our data show that paleowater temperature ranged from 5.6–21.3 °C (with 2σ values ranging from 0.2–4.8 °C), which suggest a close correlation with atmospheric temperatures around the lake. These results are in good agreement with a modern mean winter temperature (3.5 °C) and mean summer temperature (20°C) recorded in the area between 1970 and 1980.

Introduction

Quaternary deposits of north-central Mexico are poorly understood, but are significant to our understanding of past climatic change and the paleoenvironmental history of the Chihuahuan Desert and adjacent Madrean Evergreen Woodland (Brown, 1994), where the Babícora Basin is located. The Chihuahuan Desert covers a large area in the States of Chihuahua, Durango,

Coahuila, Zacatecas and San Luis Potosí (Mexico) and parts of Texas, New Mexico and Arizona (USA). The Madrean Evergreen Woodland covers the highlands of the Sierra Madre Occidental separating the Chihuahuan Desert (east) from the Sonoran Desert (west) from Trans Pecos Texas, New Mexico and Arizona (north-westward to Yavapai County) to the north, to eastern Sonora and Sinaloa and western Chihuahua and Durango (Brown, 1994).

The paleoenvironmental reconstruction of Laguna Babicora, Chihuahua is of particular interest because the site is located at the southernmost edge of the North American jet stream pathway (COHMAP, 1988). The purpose of this study is threefold: first, to interpret lake water temperature and salinity based on ostracode paleoecology and trace element shell chemistry. Second to define the Pleistocene-Holocene transition and third, based upon a combination of our results in this study and those on the sedimentology and radiocarbon chronology previously established (Ortega-Ramírez et al., 1998) to elaborate on the evolution of Laguna Babicora over the past ~ 25,000 years.

Evidence of climatic variation throughout the Chihuahuan Desert and Madrean Evergreen Woodland in the United States and occasionally northern Mexico since the late Pleistocene, has been reported elsewhere. Ortega-Ramírez et al. (1998) summarize the research conducted to date to understanding the dynamics of past climate in the area. Among the most significant approaches are paleoenvironmental studies based on: (1) macrobotanical remains and pollen from packrat middens in southwestern United States (e.g., Van Devender & Spaulding, 1979; Thompson et al., 1993); (2) palynologic studies in northern Coahuila (Meyer, 1973) and northern Durango (Van Devender & Burgess, 1985); (3) sedimentologic analysis (Ortega-Ramírez, 1990, 1995a; Urrutia-Fucugauchi et al., 1997) and; (4) climatic models (COHMAP, 1988). The results of these approaches suggest that the Chihuahuan Desert was subject to various stages of cold/wet, warm/dry conditions during the late Pleistocene that eventually evolved into the modern climate characteristic of the region.

Atmospheric circulation models developed for the late Wisconsin indicate that the westerly jet stream and the associated low pressure cells migrated south of the 30°N latitude, causing an increase in winter precipitation (Kutzbach & Wright, 1985; COHMAP, 1989). This is consistent with the occurrence of *Pinus cembroides* or *P. remota*, *Juniperus* and *Quercus* or Chaparral-type communities at relatively low elevations (600–1675 m asl) or latitudes (Bolsón de Mapimí, 26°N) (Wells, 1996; Van Devender & Burgess, 1985; Van Devender, 1990; Thompson et al., 1993). During the Holocene, the Chihuahuan Desert gradually became more arid both in the American southwest and northern Mexico (e.g. Van Devender, 1977; Markgraf et al., 1984; Van Devender et al., 1987; Elias & Van Devender, 1990; Ortega-Ramírez et al., 1998) with short intervals of relative mesic conditions (Waters, 1989; Tommey et al., 1993). To the best of our knowledge, no lacustrine

ostracode reports are available from northern Mexico.

Ostracodes are microscopic crustaceans provided with a calcite carapace. These organisms range in size from 0.5 to 2 mm. As arthropods, they shed their skeleton (8–9 molts) to complete their life cycle. Ostracodes can be highly sensitive to environmental change. Some species are cosmopolitan and occur in a variety of water chemistries and temperatures (eurytopic), whereas other species are restricted to specific environments (stenotopic). Ostracodes may occur in permanent or ephemeral water bodies and this characteristic will play a significant role in the length of their life cycle. Some species may take over a year to reach maturity (e.g., *Darwinula stevensoni*), while others require only 4–6 weeks (e.g., *Limnocythere staplini*, *Cypridopsis vidua*). By using the known environmental tolerance of several ostracode species, Delorme (1969, 1989) utilized these organisms as paleoenvironmental indicators in Canada and northern United States. Forester (1983, 1987, 1991) demonstrated that several species have specific hydrochemical requirements, thus their environmental preferences range from freshwater to alkaline or non-alkaline waters in continental aquatic ecosystems as a function of the anion composition of the water body.

Chivas et al. (1983, 1986a, b, 1993) conducted experiments with endemic Australian ostracodes, (*Australocypris/Mytilocypris*), examining the relationship between ostracode shell chemistry and water chemistry. Their results showed that Mg uptake by ostracodes is dependent on both water temperature and the Mg/Ca ratio of the host water, whereas Sr uptake is only dependent on the Sr/Ca ratio of the water. Similarly, Engstrom & Nelson (1991) recognized a relationship between ostracode shell chemistry and the host water using a ubiquitous North American species (*Candona rawsoni*). Their study indicates, however, that the Mg/Ca ratio in ostracodes is a direct function of salinity as a function of the Mg/Ca of the water. In addition, their Sr/Ca ratios in ostracodes are a poor indicator of salinity due to the weak relationship between the Sr/Ca of the water and salinity in Devils Lake.

In contrast, Palacios-Fest (1996) and Palacios-Fest and Dettman (in press) conducted experiments using widespread species of the genera *Limnocythere* (*L. staplini*) and *Cypridopsis* (*Cypridopsis vidua*). Those results indicate the Mg uptake is closely related to other environmental conditions of the water body, regardless of the Mg/Ca ratio of the host water. Palacios-Fest and Dettman (in press) demonstrated that an alternative method to calculate paleotemperature does not require

the thermodynamic equilibrium model since ostracode valves are not crystals of calcite but skeletons; therefore, they propose that Mg uptake is a biokinetic process (Palacios-Fest, 1996; Palacios-Fest & Dettman, in press).

Palacios-Fest (1996) developed standard coefficients to convert ostracode Mg/Ca ratios into paleotemperature estimates, respectively. Later, Palacios-Fest and Dettman (in press) generated standard coefficients to calculate temperatures for *C. vidua* and redefined the equation for *L. staplini*. The latter is used in this study. Wansard (1996) applied a similar model for *Cyprideis torosa* in NE Spain. Xia et al. (1997) studied the shell chemistry of *C. rawsoni* from two hypersaline lakes in the American midwest and found that the trace element ratios vary widely within the same assemblage, probably reflecting seasonal variation. De Deckker et al. (1999) cultured specimens of *Cyprideis australiensis* and found a strong thermodependence for Mg and a minor one for Sr. The Mg/Ca and Sr/Ca of the valves also showed a strong relationship with those ratios in the water, reinforcing the current hypothesis that thermodynamic equilibrium controls mineral uptake by ostracodes.

Based upon earlier studies, Palacios-Fest et al. (1994) used ostracode shell chemistry to reconstruct the paleoenvironmental history of paleolake Chewaucan, a late Pleistocene lacustrine basin today known as Summer Lake, Oregon. More recently, Palacios-Fest (1997) applied these standard coefficients to *L. staplini* from Native-American irrigation canals in the Phoenix Basin (see methodology section for description). Temperature estimates obtained from these canals are consistent with historic records from the vicinity of Phoenix from 1876 to 1995, suggesting that the standards are applicable to ancient deposits. Cohen et al. (2000) and Enzel et al. (unpublished data) have also successfully applied these coefficients to *L. cerio-tuberosa* from paleolake Chewaucan, Oregon, and Laguna Diablo, northern Baja California, Mexico, respectively.

Geologic and geographic setting

Laguna Babicora, in the State of Chihuahua, is located in an intermontane basin (29° 15'–29° 30'N and 107° 40'–108° W; 2,200 m above sea level (m asl)) in the Madrean Evergreen Woodland of the Sierra Madre Occidental (Brown, 1994) (Figure 1). The study area falls within the Basin and Range physiographic prov-

ince of western North America (Ortega-Ramírez, 1990). The basin trends NW-SE and has an area of 1,896 km², it is surrounded by hills and peaks that reach altitudes from 2,500–3,195 m asl, and consist of rhyolitic and basaltic rocks ranging in age from Miocene to Pleistocene (Ortega-Ramírez, 1990). The lake was formed in a graben that gradually filled, leaving no evidence of terrace or playa deposits. Most of the sediments are of fluvial and lacustrine origin, suggesting that from the end of the Pleistocene the morphodynamics of the area was more active than today. Runoff during wet periods created 'arroyos' in the Babicora watershed and warm/dry intervals favored deflation and poorly developed soils (horizons A0–A1 and A/C) due to decreasing precipitation (ca. 400 mm/yr) and lack of vegetation (Ortega-Ramírez, 1995a).

Today, the annual mean precipitation is about 450 mm and the mean annual temperature is 11.5 °C (Ortega-Ramírez et al., 1998). Following Köppen's climate classification, the region's climate is characterized by cold winters (mean temperature of 3.5 °C) and hot and humid summers (mean temperature 20°C) (García, 1973). Air mass circulation in the summer is dominated by air fluxes from the east, whereas, during the winter, air fluxes move from the west and are associated with the high atmosphere jet stream (Brisson & Lowry, 1955; Hales, 1974; Nelson, 1986).

In response to this climatic pattern the regional vegetation forms three distinctive zones: (1) montane conifer forest above 2,400 m, (2) juniper-oak woodland, from 2,400 to 2,200 m, and (3) arid tropical scrub dominated by grassland below 2,200 m (Ortega-Ramírez, 1995a). Powell and Hilsenbeck (1995) characterized Laguna Babicora as a mesic ecosystem isolated by surrounding desert habitats. Madrean Evergreen Woodland occurs above or within the drier interior chaparral, and below and along drainages from the mountains in Chihuahua and Coahuila to the drier and more cold tolerant Great Basin conifer woodland (Brown, 1994). Currently, Laguna Babicora is a dry playa but occasionally inundates during heavy storms.

Methods

Outcrop and test pit profiles in Laguna Babicora were made in 1992. Three of the eight profiles were selected for this study based on previous results (Ortega-Ramírez, 1990, 1995a, b; Urrutia-Fucugauchi et al., 1997; Ortega-Ramírez et al., 1998). The El Diablo profile (outcrop) is located at the south end of the Laguna

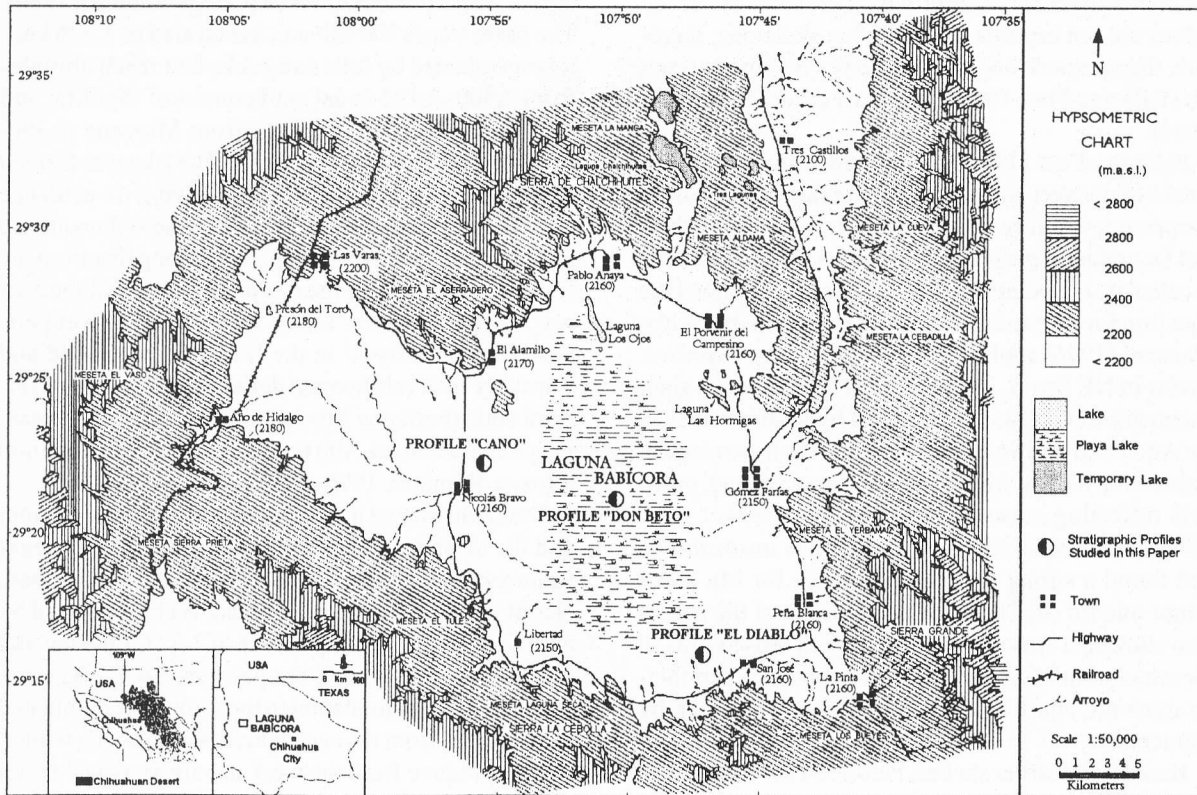


Figure 1. Location map of Laguna Babicora, Chihuahua, Mexico.

Babicora basin and provided 23 samples (depth of 243 cm). The Don Beto profile (test pit), at the lake's depocenter, consisted of 14 samples (depth of 230 cm). The Cano-Magallanes profile (outcrop), near the western shoreline, included 18 samples (depth of 298 cm). Samples were collected at variable stratigraphic spacing. Ortega-Ramírez (1995a) and Ortega-Ramírez et al. (1998) described the sedimentological procedures of the data used in this study. All three profiles were studied for a variety of proxy records and correlation tools, including granulometry, sediment composition, ostracode paleoecology, stratigraphy, and shell chemistry.

Sedimentologically, the three profiles used for this study (El Diablo, Don Beto and Cano Magallanes) were similar, with some minor differences derived from their geomorphologic and topographic positions within the basin (Figure 2). Table 1 lists the radiocarbon dates obtained.

El Diablo profile (2.5 m long) consists of four distinct lithostratigraphic units. Unit IV is a brownish-gray sand and silt. Unit II is a gray fine sand with abundant ostracodes and an irregular basal contact (16,342 ±

200 yrs B.P. at 166 cm). Unit II is a thin-bedded, grayish-brown silty clay which is stratified with a sharp depositional contact at the base (10,976 ± 115 yrs B.P. at 100 cm). Unit I is a thin-bedded, brown silty sand with abundant organic matter; it is horizontally stratified with a transitional contact at its base (4,345 ± 105 yrs B.P. at 59 cm).

Don Beto profile, approximately 2.3 m long, has two lithostratigraphic units. Unit II is a grayish-brown clayey silt occasionally alternating with silty clay and sandy-silty clay layers (24,470 ± 765 yrs B.P. at 230 cm and 11,885 ± 315 yrs B.P. at 140 cm). Unit I is a light brown silty clay (1,300 ± 65 yrs B.P. at 35 cm).

Cano Magallanes profile, 2.98 m long, consists of three lithostratigraphic units. Unit III is a yellowish-red fluvial gravelly sand. Unit II is a composite sequence of dark brown to yellowish-brown sandy clay, silty clay and fine sand with a transitional contact at the base (9,614 ± 130 yrs B.P. at 168 cm). Unit I is a thick-bedded, black organic silty clay, stratified and with a sharp basal contact (7,965 ± 109 yrs B.P. at 78 cm and 3,503 ± 101 yrs B.P. at 43 cm).

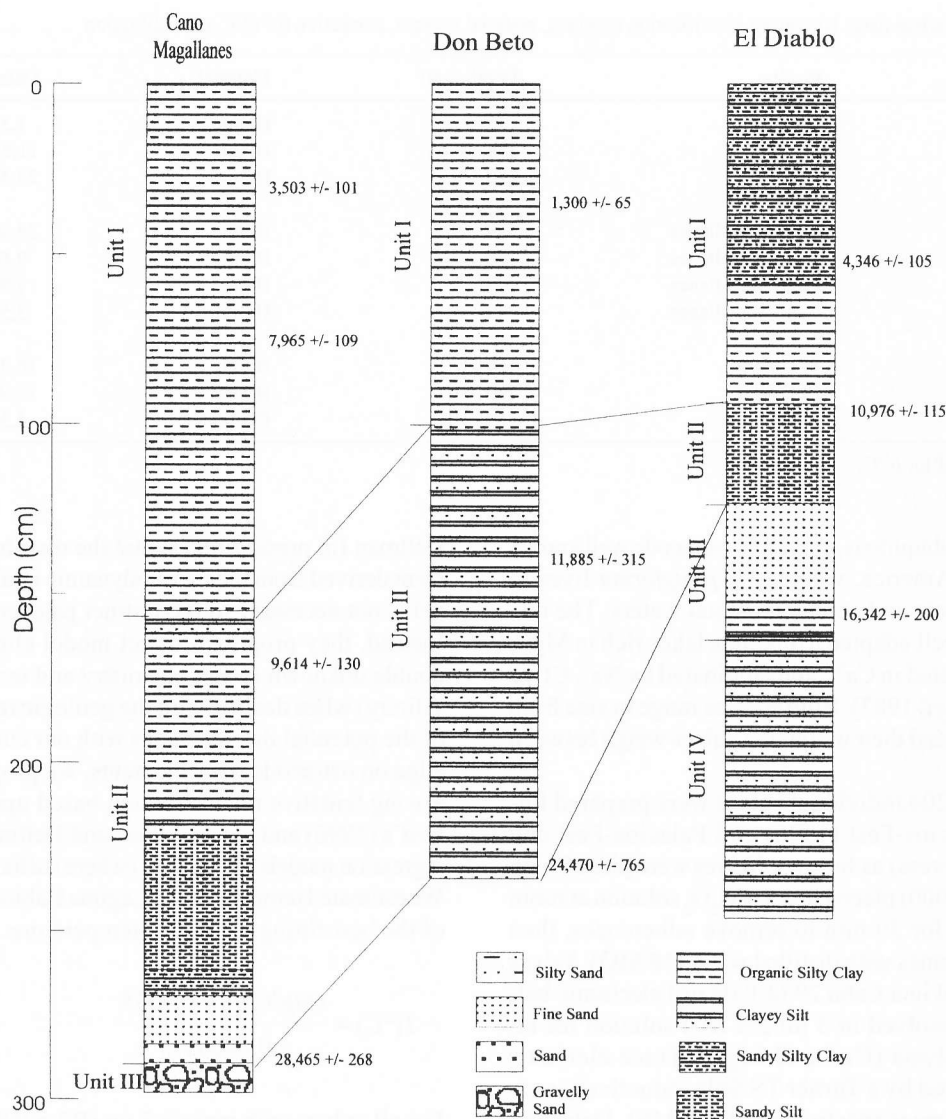


Figure 2. Stratigraphic correlation among the three profiles used in this study.

Routine micropaleontological sample preparation was conducted on the 56 sediment samples. All samples were initially weighed, washed, and screened through a set of two stacked sieves (> 106 and $> 63 \mu\text{m}$) to remove fine sediments. The residues were also weighed and then analyzed using a low power stereoscopic microscope. Forty-three samples were fossiliferous. Ostracode species were identified, and a reference collection was prepared from each horizon. Based upon the fossiliferous contents, faunal assemblages were determined to establish paleoecologic trends and a paleosalinity index using the equation of Palacios-Fest et al. (1993):

$$\text{Paleosalinity Index (SI)} = [4(\textit{Limnocythere sappaensis}) + 3(\textit{Limnocythere ceriotuberosa}) + 2(\textit{Limnocythere bradburyi}) + (\textit{Cypridopsis vidua})] - [(\textit{Candona caudata}) + 2(\textit{Candona patzcuaro}) + 3(\textit{Limnocythere platyforma})] \quad (1)$$

where species with incrementally higher salinity tolerances are weighted positively and species with incrementally lower salinity tolerances are weighted negatively.

Limnocythere ceriotuberosa and *L. platyforma*, the two most common species present in Laguna Babicora were chosen for the shell chemistry analysis. *L. cerio-*

Table 1. Radiocarbon dates laboratory identification numbers, material sources, correction for $\delta^{13}\text{C}$ and calibration

Laboratory #	Profile	Depth (cm)	Material	Date (yrs B.P.)
*A-8392	Don Beto	35	Humic	1,300 \pm 65
*A-8393	Don Beto	134	Humic	11,885 \pm 315
*A-8394	Don Beto	230	Humic	24,470 \pm 765
INAH-1208	Cano Magallanes	279	Humic	28,465 \pm 268
INAH-1209	Cano Magallanes	168	Humic	9,614 \pm 130
INAH-1210	Cano Magallanes	78	Humic	7,965 \pm 109
INAH-1211	Cano Magallanes	43	Humic	3,503 \pm 101
INAH-1212	El Diablo	166	Humic	16,342 \pm 201
INAH-1214	El Diablo	100	Humic	10,976 \pm 115
INAH-1215	El Diablo	59	Charcoal	4,346 \pm 105

*Dates corrected for $\delta^{13}\text{C}$.

tuberosa is a ubiquitous, eurytopic ostracode well known from North America, whereas *L. platyforma* lives in relatively dilute and cold continental waters. The two species are well adapted to alkaline lakes rich in Mg^{2+} , slightly depleted in Ca^{2+} , and dominated by Na^+ , Cl^- or SO_4^{2-} (Forester, 1983). Both species range in size from 600–800 μm and their individual valves weigh between 5 and 10 μg .

A total of 204 individual valves were prepared following Palacios-Fest (1996) and Palacios-Fest and Dettman (in press) as follows: Valves were picked with a fine brush (000) placed in a 5% H_2O_2 solution at room temperature for 30 min to remove adherences, then rinsed three times with distilled water (18 M Ω). Valves were weighed in a Cahn 29 (\pm 0.02 μg) electronic balance, and dissolved in 3 ml 2% HCl solution for elemental analysis (Ca^{2+} and Mg^{2+}). Trace elements were measured by a Turner TS Sola inductively coupled plasma mass spectrometer (ICP-MS). Detection limits for Mg^{2+} were 0.001 $\mu\text{g l}^{-1}$ and 10 $\mu\text{g l}^{-1}$ for Ca^{2+} – 2 σ above background. All analyses were run against multi-element standards prepared from SpexTM stock solutions. In order to obtain good counting statistics four scans were made per sample, with four passes per scan, consuming the whole sample. Precision is 3% of signal for Mg^{2+} and 6% of signal for Ca^{2+} (2 σ). Due to ^{40}Ar interference, we preferred to calculate Ca^{2+} content stoichiometrically.

Environmental reconstructions based on ostracode trace elements have proven a difficult task as suggested by De Deckker et al. (1999). Their work shows the strong relationship between the Me/Ca ratios of the valves and those of the water, hence showing the strong thermodynamic equilibrium effect on mineral uptake. In contrast, Palacios-Fest (1996) and Palacios-Fest and

Dettman (in press) suggest that the distribution coefficient derived from the thermodynamic equilibrium model is not necessary to reconstruct paleoenvironments. Instead, they propose a direct model eliminating the double unknown (water chemistry and temperature or salinity) when dealing with the geologic record. Aware of the potential discrepancies with our current knowledge on ostracode trace elements, we propose the following tentative reconstruction based upon Palacios-Fest's (1996) and Palacios-Fest and Dettman (in press) regression models for Mg/Ca_v (where suffix 'v' = valve). We estimated temperature of Laguna Babicora by means of the best fitting model for temperature.

$$T(^{\circ}\text{C}) = \frac{(\text{Mg}/\text{Ca}_v) + 0.0035}{0.00089} \quad (2)$$

For all valves with mass > 3 μg ($R^2 = 0.997$).

Results

Ostracode paleoecology

Figure 3 summarizes ostracode paleoecology, total and relative species abundance and the paleosalinity index (SI). Ostracode diversity is low in Laguna Babicora, but number of valves range from extremely low (1) to extremely high (4,505). Four species of the genus *Limnocythere* occur in this lake; *L. bradburyi*, *L. ceriotuberosa*, *L. platyforma* and *L. sappaensis*. Other species present are *Candona patzcuaro*, *Candona caudata*, and *Cypridopsis vidua*. The most common and abundant species throughout the record are *L.*

ceriotuberosa and *C. patzcuaro* followed by *L. sappensis*, and in some intervals, *L. platyforma* or *L. bradburyi*.

Based on the relative abundance of these species, three assemblages (I–III) are recognized (Table 2); all of which characterize Water Pathway Types I and III

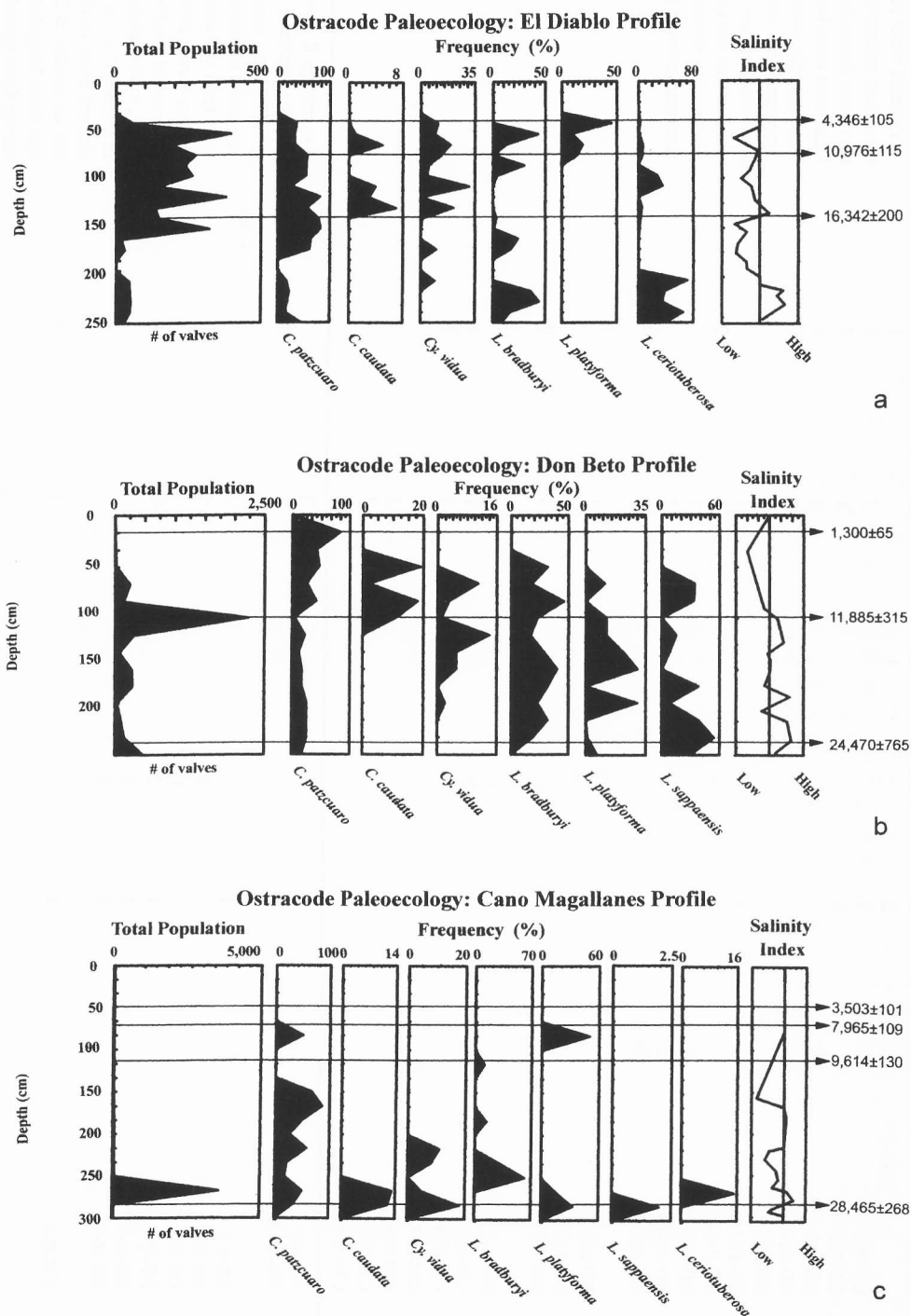


Figure 3. Ostracode paleoecology and stratigraphy from the three profiles: (a) El Diablo, (b) Don Beto and, (c) Cano Magallanes. Diagrams are arranged, from left to right, as follows: total population indicating ^{14}C dates, relative abundance by species and salinity index derived from equation (1).

Table 2. Continued

Assemblage	Sample	<i>L. sappaensis</i>	<i>L. ceriotuberosa</i>	<i>L. bradburyi</i>	<i>L. platyforma</i>	<i>Candona caudata</i>	<i>Candona patzcuaro</i>	<i>Cypridopsis vidua</i>	Environment
III	ED-IV-2		1	2		2			Assemblage III represents saline water conditions. Lake level dropped substantially during these intervals. Water temperature and salinity fluctuated significantly. El Diablo profile showed a 'continuous' ostracode record which could be associated with water discharge to the lake. Cano Magallanes profile, instead, showed extremely ephemeral conditions from 220 cm to the top, suggesting lake desiccation. At Don Beto profile the lake was permanent. Saline conditions indicate P < E.
	ED-IV-3		1	1		2			
	ED-IV-4		1	1		2			
	ED-IV-5		1				2	3	
	DB-I-1	2		1		4	3	4	
	DB-I-2	1		2	3	2	4	3	
	DB-II-2	2		1	4		3		
	DB-II-3	1		2			3		
	DB-II-5	2		1			3		
	CM-II-2			1			2		
	CM-II-10			1					

(HCO₃⁻-enriched water dominated additionally by Na⁺, Mg²⁺ and SO₄²⁻) of Eugster and Hardie (1978). INEGI's (1990) water analysis from 26 wells and a spring in the Babicora Basin show relatively high concentrations of HCO₃⁻ (104.1 mg l⁻¹), Na⁺ (77.4 mg l⁻¹), Mg²⁺ (26.2 mg l⁻¹) and SO₄²⁻ (177.3 mg l⁻¹) and low Ca²⁺ (31.8 mg l⁻¹), consistent with ostracode assemblages.

Ostracode assemblages are defined by species association and dominant group. Assemblage I is represented by freshwater species either dominated by *Candona patzcuaro* or *Limnocythere platyforma*; eurytopic species may be present. Assemblage II is characterized by near-equal proportions of either fresh- or saline-water species (*Candona patzcuaro*/*Limnocythere platyforma*, the freshwater indicators; or *L. sappaensis*, *L. ceriotuberosa* and *L. bradburyi*, the saline indicators), reflecting an environmental transition. Assemblage III is formed by salinity-tolerant species dominated by three species of the genus *Limnocythere* (*L. sappaensis*, *L. ceriotuberosa* and *L. bradburyi*).

The qualitative paleosalinity index derived from each one of the three profiles show frequent salinity fluctuations. Figure 3a suggests that at its southern end (El Diablo), Laguna Babicora was more saline at the base of the record but gradually became fresher with occasional saline phases. In contrast, Figure 3b indicates that at its depocenter (Don Beto) the lake remained more saline as a result of ionic concentration, but salinity declined toward the end of the record. The short record of Cano Magallanes (Figure 3c) shows that the western-end of the lake remained mostly fresh with only occasional slightly saline incursions. Freshwater conditions probably resulted from frequent runoff through the alluvial fan (*bagajada*).

Ostracode shell chemistry

Figure 4 and Tables 3 and 4 summarize the shell chemistry of *Limnocythere*, inferred temperature records. Mg/Ca_s values from Laguna Babicora ostracodes follow a similar trend to those values obtained from experimental specimens. Temperature (°C) estimates derived using Palacios-Fest (1996) and Palacios-Fest and Dettman (in press) standard coefficients are in good agreement with modern seasonal atmospheric temperatures recorded from the area over the past 20 years (Ortega-Ramirez et al., 1998). Today, Laguna Babicora is a dry playa and no living ostracodes occur in the basin.

The apparent low values of Mg/Ca_s are consistent with values recorded elsewhere for other species (Engstrom

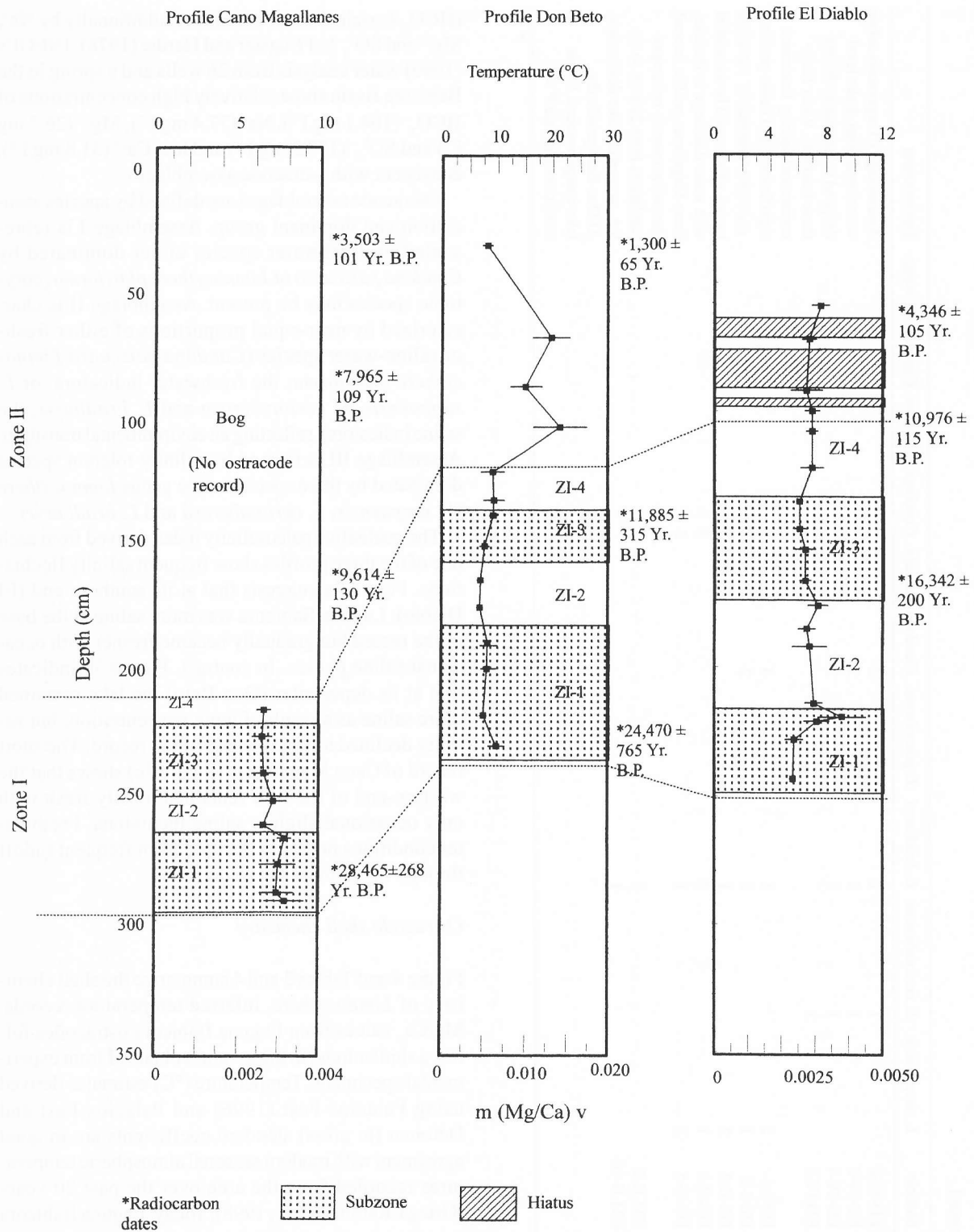


Figure 4. Reconstruction of paleotemperature records based on the Mg/Ca_v values obtained from *Limnocythere ceriotuberosa* and *L. platyforma* at all three profiles. Two zones and a maximum of four sub-zones for Zone I were identified at Laguna Babicora. During the Holocene at El Diablo three erosional or non-depositional events were evident. At this time, as the lake shrank, it formed a bog to the west (Cano Magallanes). 2σ error bars and ¹⁴C dates are included for each profile.

Table 3. *Limnocythere* shell chemistry documenting measured concentrations of Ca²⁺ and Mg²⁺ through ICP-MS, from (a) El Diablo Profile, (b) Don Beto Profile and, (c) Cano Magallanes Profile. Notice that Ca²⁺ content was calculated stoichiometrically

Laguna Babicoora, Chibuhuan													
Profile	Sequence #	Depth (cm)	Age (Years B.P.)	Sample #	Replicate	Valve Wt. (µg)	Ca* (ng/ml in sol)	Mg	Ca* (µg)	Mg	Mg ppm	Ca* (mol)	Mg
El Diablo	115	59	4346±105	ED-I-3	A	8.9	3548.17	8.81	3.55	0.009	990	8.8E-11	3.6E-13
	116				B	13.7	5728.44	10.52	5.47	0.010	733	1.4E-10	4.1E-13
	117				C	12.2	4837.43	9.40	4.86	0.009	775	1.2E-10	3.9E-13
	118				D	15.5	6168.38	12.34	6.18	0.012	798	1.5E-10	5.1E-13
	119				E	13.4	5335.82	8.93	5.33	0.009	668	1.3E-10	3.7E-13
	120	72		ED-I-2	A	10.9	4652.23	6.44	4.35	0.006	553	1.1E-10	2.5E-13
	121				B	14.0	5648.84	9.95	5.59	0.010	703	1.4E-10	4.1E-13
	122				C	11.8	4773.88	7.92	4.71	0.008	662	1.2E-10	3.2E-13
	123				D	14.8	6333.58	7.89	5.91	0.007	498	1.5E-10	3.0E-13
	124				E	11.4	4751.70	8.54	4.55	0.008	717	1.1E-10	3.4E-13
	125	92		ED-I-1	A	12.8	5132.47	10.89	5.11	0.011	846	1.3E-10	4.5E-13
	126				B	9.2	3641.08	2.81	3.68	0.003	309	9.2E-11	1.2E-13
	127				C	13.9	5887.71	4.92	5.56	0.005	334	1.4E-10	1.9E-13
	128				D	11.2	4484.94	6.55	4.47	0.007	583	1.1E-10	2.7E-13
	129				E	12.6	5122.11	9.73	5.03	0.010	758	1.3E-10	3.9E-13
	130	100	10976±115	ED-II-3	A	14.0	5770.55	11.26	5.59	0.011	779	1.4E-10	4.5E-13
	131				B	13.9	5844.91	10.03	5.55	0.010	685	1.4E-10	3.9E-13
	132				C	14.0	5890.24	8.33	5.59	0.008	565	1.4E-10	3.3E-13
	133				D	12.1	4783.52	6.14	4.83	0.006	513	1.2E-10	2.6E-13
	134				E	13.0	5791.36	10.63	5.19	0.010	733	1.3E-10	3.9E-13
	135	108		ED-II-2	A	14.0	5761.14	7.83	5.59	0.008	543	1.4E-10	3.1E-13
	136				B	13.0	5174.67	9.45	5.19	0.009	729	1.3E-10	3.9E-13
	137				C	11.5	4691.29	7.58	4.59	0.007	645	1.1E-10	3.1E-13
	138				D	13.9	5651.65	11.22	5.55	0.011	792	1.4E-10	4.5E-13
	139				E	10.5	4284.67	6.72	4.19	0.007	626	1.0E-10	2.7E-13
	140	122		ED-II-1	A	12.3	4943.77	11.83	4.90	0.012	954	1.2E-10	4.8E-13
	141				B	10.5	4237.86	6.64	4.19	0.007	626	1.0E-10	2.7E-13
	142				C	10.8	4361.60	5.72	4.32	0.006	524	1.1E-10	2.3E-13
	143				D	12.0	4792.80	7.22	4.79	0.007	602	1.2E-10	3.0E-13
	144				E	12.4	5102.52	7.27	4.95	0.007	569	1.2E-10	2.9E-13
	145	135		ED-III-3	A	15.5	6414.70	8.68	6.19	0.008	541	1.5E-10	3.4E-13
	146				B	14.9	6325.21	7.36	5.95	0.007	465	1.5E-10	2.9E-13
	147				C	15.0	6313.35	7.96	5.99	0.008	504	1.5E-10	3.1E-13
	148				D	14.9	6153.20	6.14	5.96	0.006	399	1.5E-10	2.4E-13
	149				E	26.4	11600.85	13.95	10.55	0.013	481	2.6E-10	5.2E-13
	150	146		ED-III-2	A	12.9	5112.08	7.40	5.15	0.007	578	1.3E-10	3.1E-13
	151				B	14.6	5899.25	6.07	5.84	0.006	411	1.5E-10	2.5E-13
	152				C	15.0	6042.94	7.07	5.99	0.007	468	1.5E-10	2.9E-13
	153				D	12.4	5038.61	4.67	4.96	0.005	371	1.2E-10	1.9E-13
	154				E	14.8	5880.67	7.93	5.91	0.008	539	1.5E-10	3.3E-13
	155	154		ED-III-1	A	12.9	5150.90	8.45	5.15	0.008	655	1.3E-10	3.5E-13
	156				B	14.9	5140.76	8.14	5.95	0.009	632	1.5E-10	3.9E-13
	157				C	14.4	6039.40	10.37	5.75	0.010	686	1.4E-10	4.1E-13
	158				D	15.7	6325.74	6.91	6.28	0.007	437	1.6E-10	2.8E-13
	159				E	12.8	5186.93	4.88	5.12	0.005	376	1.3E-10	2.0E-13
	160	166	16342±200	ED-IV-11	A	8.2	3347.62	4.53	3.28	0.004	541	8.2E-11	1.8E-13
	161				B	9.9	4095.56	6.10	3.95	0.006	595	9.9E-11	2.4E-13
	162				C	8.3	3353.54	3.59	3.32	0.004	428	8.3E-11	1.5E-13
	163				D	10.7	4240.62	5.97	4.27	0.006	562	1.1E-10	2.5E-13
	164				E	8.7	3419.19	5.62	3.47	0.006	656	8.7E-11	2.3E-13
	165	176		ED-IV-10	A	11.5	4556.09	7.09	4.59	0.007	621	1.1E-10	2.9E-13
	166				B	9.5	3835.48	5.69	3.79	0.006	593	9.5E-11	2.3E-13
	167				C	7.5	3117.88	5.67	2.99	0.005	726	7.5E-11	2.2E-13
	168				D	6.6	2550.83	5.65	2.63	0.006	883	6.6E-11	2.4E-13
	169				E	6.0	2451.98	5.61	2.39	0.005	913	6.0E-11	2.3E-13
	170	185		ED-IV-9	A	6.2	2516.83	3.73	2.48	0.004	592	6.2E-11	1.5E-13
	171				B	12.8	5329.07	5.94	5.12	0.006	446	1.3E-10	2.3E-13
	172				C	7.6	3164.43	3.27	3.04	0.003	413	7.6E-11	1.3E-13
	173				D	7.8	2890.65	4.96	3.11	0.005	685	7.8E-11	2.2E-13
	174				E	8.3	2923.58	5.03	3.31	0.006	687	8.3E-11	2.3E-13
	175	192		ED-IV-8	A	9.8	4145.49	6.50	3.91	0.006	626	9.8E-11	2.5E-13
	176				B	9.7	3982.49	4.77	3.88	0.005	479	9.7E-11	1.9E-13
	177				C	3.8	1513.82	4.06	1.51	0.004	1068	3.8E-11	1.7E-13
	178				D	7.1	2939.36	2.82	2.84	0.003	383	7.1E-11	1.1E-13
	179				E	9.6	4039.82	5.30	3.84	0.005	524	9.6E-11	2.1E-13
	180	214		ED-IV-5	A	6.7	2681.97	4.51	2.67	0.004	671	6.7E-11	1.9E-13
	181				B	9.9	4062.65	5.16	3.95	0.005	509	9.9E-11	2.1E-13
	182				C	7.2	2960.70	5.09	2.87	0.005	686	7.2E-11	2.0E-13
	183				D	7.7	3066.03	4.95	3.07	0.005	645	7.7E-11	2.0E-13
	184				E	4.7	1879.44	4.17	1.87	0.004	885	4.7E-11	1.7E-13
	185	219		ED-IV-4	A	7.0	2732.52	10.74	2.78	0.011	1563	6.9E-11	4.5E-13
	186				B	6.1	2389.22	4.59	2.43	0.005	767	6.1E-11	1.9E-13
	187				C	4.2	1663.30	5.28	1.67	0.005	1264	4.2E-11	2.2E-13
	188				D	5.3	2287.99	6.96	2.11	0.006	1212	5.3E-11	2.6E-13
	189				E	6.4	2494.69	4.37	2.55	0.004	699	6.4E-11	1.8E-13
	190	221		ED-IV-3	A	7.8	3123.62	3.84	3.12	0.004	491	7.8E-11	1.6E-13
	191				B	7.2	2952.15	4.99	2.87	0.005	675	7.2E-11	2.0E-13
	192				C	4.0	1615.50	4.03	1.59	0.004	994	4.0E-11	1.6E-13

Table 3. Continued

Profile	Sequence #	Depth (cm)	Age (Years B.P.)	Sample #	Replicate	Valve Wt. (µg)	Ca* (ng/ml in sol)	Mg	Ca* (µg)	Mg	Mg	Ca* (mol)	Mg
	193				D	8.9	3720.51	6.40	3.55	0.006	687	8.9E-11	2.5E-13
	194				E	5.2	2184.99	4.26	2.07	0.004	778	5.2E-11	1.7E-13
	195	228		ED-IV-2	A	8.4	3390.48	5.25	3.35	0.005	618	8.4E-11	2.1E-13
	196				B	13.4	5611.40	5.02	5.36	0.005	358	1.3E-10	2.0E-13
	197				C	13.0	5459.61	4.68	5.20	0.004	343	1.3E-10	1.8E-13
	198				D	12.0	4811.22	3.93	4.80	0.004	327	1.2E-10	1.6E-13
	199				E	15.9	6795.27	4.62	6.36	0.004	272	1.6E-10	1.8E-13
	200	243		ED-IV-1	A	13.9	5485.94	4.33	5.56	0.004	316	1.4E-10	1.8E-13
	201				B	13.0	4640.22	4.78	5.20	0.005	412	1.3E-10	2.2E-13
	202				C	13.1	5307.73	5.21	5.24	0.005	392	1.3E-10	2.1E-13
	203				D	14.7	6039.90	4.63	5.88	0.005	307	1.5E-10	1.9E-13
	204				E	11.6	4552.52	4.55	4.64	0.005	400	1.2E-10	1.9E-13
Don Beto													
	111	35	1300±65	DB-I-5	A	6.9	2539.03	7.00	2.75	0.008	1098	6.9E-11	3.1E-13
	112				B	16.8	7079.58	14.90	6.70	0.014	840	1.7E-10	5.8E-13
	113				C	15.8	6569.85	11.38	6.31	0.011	691	1.6E-10	4.5E-13
	114				D	6.9	2597.40	6.66	2.75	0.007	1022	6.9E-11	2.9E-13
	106	71		DB-I-4	A	12.8	4919.42	35.45	5.06	0.036	2851	1.3E-10	1.5E-12
	107				B	14.2	5849.16	43.65	5.62	0.042	2951	1.4E-10	1.7E-12
	108				C	16.9	6862.90	75.82	6.64	0.073	4343	1.7E-10	3.0E-12
	109				D	22.1							
	110				E	22.6	8624.56	72.19	8.92	0.075	3305	2.2E-10	3.1E-12
	101	90		DB-I-3	A	22.1	9629.56	25.87	8.81	0.024	1071	2.2E-10	9.7E-13
	102				B	15.9	7423.39	50.70	6.30	0.043	2704	1.6E-10	1.8E-12
	103				C	25.5	10830.94	64.46	10.11	0.060	2359	2.5E-10	2.5E-12
	104				D	18.2	7663.00	46.96	7.21	0.044	2429	1.8E-10	1.8E-12
	105				E	15.1	6559.25	53.58	5.96	0.049	3227	1.5E-10	2.0E-12
	96	106		DB-I-2	A	13.3	5258.11	68.94	5.20	0.068	5128	1.3E-10	2.8E-12
	97				B	9.6	3875.20	40.52	3.77	0.039	4108	9.4E-11	1.6E-12
	98				C	12.8	5028.78	47.64	5.04	0.048	3732	1.3E-10	2.0E-12
	99				D	10.9	4597.62	29.97	4.32	0.028	2581	1.1E-10	1.2E-12
	100				E	12.1	4819.06	35.49	4.78	0.035	2910	1.2E-10	1.4E-12
	91	123		DB-I-1	A	14.0	6211.95	15.68	5.58	0.014	1007	1.4E-10	5.8E-13
	92				B	8.1							
	93				C	8.9							
	94				D	21.1	9919.04	19.74	8.41	0.017	793	2.1E-10	6.9E-13
	95				E	8.3	3605.54	14.63	3.30	0.013	1612	8.2E-11	5.5E-13
	86	134		DB-II-9	A	10.0	3911.68	10.74	3.98	0.011	1094	9.9E-11	4.5E-13
	87				B	12.8	4447.34	13.17	5.10	0.015	1180	1.3E-10	6.2E-13
	88				C	9.3	2948.94	13.05	3.70	0.016	1759	9.2E-11	6.7E-13
	89				D	14.8	7289.45	12.11	5.91	0.010	663	1.5E-10	4.0E-13
	90				E	9.1	3512.20	10.52	3.62	0.011	1193	9.0E-11	4.5E-13
	81	140	11885±315	DB-II-8	A	7.1	2903.46	10.06	2.83	0.010	1379	7.0E-11	4.0E-13
	82				B	11.4	4481.65	12.78	4.54	0.013	1136	1.1E-10	5.3E-13
	83				C	10.6	4169.28	10.64	4.22	0.011	1017	1.1E-10	4.4E-13
	84				D	9.3	3807.63	10.74	3.71	0.010	1124	9.2E-11	4.3E-13
	85				E	9.8	3624.41	9.79	3.90	0.011	1076	9.7E-11	4.3E-13
	76	152		DB-II-7	A	12.3	4579.53	7.69	4.91	0.008	670	1.2E-10	3.4E-13
	77				B	9.9	4242.53	9.07	3.95	0.008	853	9.8E-11	3.5E-13
	78				C	18.3	8189.16	22.34	7.29	0.020	1087	1.8E-10	8.2E-13
	79				D	11.8	4891.70	10.10	4.71	0.010	824	1.2E-10	4.0E-13
	80				E	10.1	4200.54	6.87	4.03	0.007	653	1.0E-10	2.7E-13
	71	165		DB-II-6	A	16.9	6933.40	10.10	6.75	0.010	582	1.7E-10	4.0E-13
	72				B	14.8	6000.15	12.23	5.90	0.012	813	1.5E-10	5.0E-13
	73				C	18.0	6911.52	9.31	7.19	0.010	538	1.8E-10	4.0E-13
	74				D	16.0	5827.42	9.20	6.39	0.010	630	1.6E-10	4.1E-13
	75				E	19.1	7462.04	13.50	7.62	0.014	722	1.9E-10	5.7E-13
	66	176		DB-II-5	A	15.7	5161.96	9.70	6.26	0.012	750	1.6E-10	4.8E-13
	67				B	21.3							
	68				C	12.8							
	69				D	17.2	6906.05	9.62	6.87	0.010	556	1.7E-10	3.9E-13
	70				E	16.9	5995.36	8.94	6.75	0.010	595	1.7E-10	4.1E-13
	61	190		DB-II-4	A	10.3	4107.13	12.74	4.10	0.013	1234	1.0E-10	5.2E-13
	62				B	21.3	6750.71	12.15	8.50	0.015	718	2.1E-10	6.3E-13
	63				C	13.8	4433.43	11.56	5.50	0.014	1039	1.4E-10	5.9E-13
	64				D	21.1	8041.39	10.30	8.43	0.011	512	2.1E-10	4.4E-13
	65				E	11.4	3657.44	10.96	4.54	0.014	1192	1.1E-10	5.6E-13
	56	200		DB-II-3	A	12.7	4904.77	12.85	5.06	0.013	1044	1.3E-10	5.5E-13
	57				B	14.7	14987.78	15.86	5.88	0.006	423	1.5E-10	2.6E-13
	58				C	15.7	7620.39	18.24	6.26	0.015	954	1.6E-10	6.2E-13
	59				D	10.0	3811.32	11.23	3.98	0.012	1174	9.9E-11	4.8E-13
	60				E	10.4	4091.38	10.22	4.15	0.010	996	1.0E-10	4.3E-13
	51	218		DB-II-2	A	13.0	5490.38	11.08	5.18	0.010	805	1.3E-10	4.3E-13
	52				B	11.9	5231.28	13.22	4.74	0.012	1007	1.2E-10	4.9E-13
	53				C	13.8	5638.44	10.22	5.50	0.010	723	1.4E-10	4.1E-13
	54				D	10.4	4118.30	7.22	4.15	0.007	700	1.0E-10	3.0E-13
	55				E	9.9	4397.57	7.88	3.95	0.007	715	9.9E-11	2.9E-13
	46	230	24470±765	DB-II-1	A	8.2	2884.08	10.90	3.26	0.012	1503	8.1E-11	5.1E-13
	47				B	7.2	2753.86	10.13	2.86	0.011	1463	7.1E-11	4.3E-13
	48				C	10.0	3680.11	9.58	3.98	0.010	1037	9.9E-11	4.3E-13
	49				D	9.8	4014.98	8.81	3.91	0.009	875	9.7E-11	3.5E-13
	50				E	5.7	2162.51	8.18	2.27	0.009	1504	5.7E-11	3.5E-13

Table 3. Continued

Profile	Sequence #	Depth (cm)	Age (Years B.P.)	Sample #	Replicate	Valve Wt. (μg)	Ca* (ng/ml in sol)	Mg	Ca* (μg)	Mg	Mg ppm	Ca (moles)	Mg
Cano Magallanes													
		36	3503 \pm 101										
		78	7965 \pm 109										
		168	9614 \pm 130										
	41	220		CM-II-8	A	12.8	5004.69	7.56	5.11	0.008	603	1.3E-10	3.2E-13
	42				B	12.9	5085.31	6.74	5.15	0.007	529	1.3E-10	2.8E-13
	43				C	10.8	4303.90	5.26	4.32	0.005	488	1.1E-10	2.2E-13
	44				D	11.0	4334.26	7.27	4.39	0.007	670	1.1E-10	3.0E-13
	45				E								
	36	230		CM-II-7	A	17.0	6975.98	10.62	6.79	0.010	608	1.7E-10	4.3E-13
	37				B	13.8	5567.32	10.88	5.51	0.011	780	1.4E-10	4.4E-13
	38				C	15.8	6689.08	7.42	6.31	0.007	443	1.6E-10	2.9E-13
	39				D	9.9	3842.59	5.16	3.96	0.005	537	9.9E-11	2.2E-13
	40				E	4.8	1845.00	2.06	1.92	0.002	446	4.8E-11	8.8E-14
	31	244		CM-II-6	A	8.9	3594.18	4.38	3.56	0.004	487	8.9E-11	1.8E-13
	32				B	10.9	4295.13	6.14	4.35	0.006	571	1.1E-10	2.6E-13
	33				C	10.9	4401.75	5.66	4.35	0.006	514	1.1E-10	2.3E-13
	34				D	12.0	5092.95	6.06	4.79	0.006	475	1.2E-10	2.3E-13
	35				E	8.1	3320.21	7.04	3.23	0.007	846	8.1E-11	2.8E-13
	26	255		CM-II-5	A	10.4	4364.67	4.83	4.16	0.005	442	1.0E-10	1.9E-13
	27				B	8.5	3475.38	6.46	3.39	0.006	742	8.5E-11	2.6E-13
	28				C	5.1	2067.93	3.65	2.03	0.004	704	5.1E-11	1.5E-13
	29				D	10.9	4068.41	6.85	4.35	0.007	672	1.1E-10	3.0E-13
	30				E	6.2	2519.34	5.89	2.47	0.006	932	6.2E-11	2.4E-13
	21	264		CM-II-4	A	7.0	2795.13	3.32	2.80	0.003	474	7.0E-11	1.4E-13
	22				B	7.8	2883.94	3.81	3.11	0.004	528	7.8E-11	1.7E-13
	23				C	8.0	3184.78	5.62	3.19	0.006	704	8.0E-11	2.3E-13
	24				D	9.3	3706.31	4.43	3.72	0.004	478	9.3E-11	1.8E-13
	25				E	9.6	3981.04	6.49	3.83	0.006	651	9.6E-11	2.6E-13
	16	269		CM-II-3	A	8.0	3316.01	6.34	3.19	0.006	763	8.0E-11	2.5E-13
	17				B	11.8							
	18				C	10.0							
	19				D	6.8	2689.25	6.17	2.71	0.006	915	6.8E-11	2.6E-13
	20				E	6.8	2646.97	5.85	2.71	0.006	881	6.8E-11	2.5E-13
	11	279		CM-II-2	A	10.9	4410.95	6.75	4.35	0.007	611	1.1E-10	2.7E-13
	12				B	10.9	4383.71	8.64	4.35	0.009	786	1.1E-10	3.5E-13
	13				C	10.8	4381.36	7.55	4.31	0.007	688	1.1E-10	3.1E-13
	14				D	9.9	4029.48	5.54	3.95	0.005	549	9.9E-11	2.2E-13
	15				E	6.1	2496.25	7.34	2.43	0.007	1171	6.1E-11	2.9E-13
	6	290			A	8.0	3050.78	3.40	3.20	0.004	445	8.0E-11	1.5E-13
	7				B	7.4	2873.57	7.03	2.95	0.007	975	7.4E-11	3.0E-13
	8				C	10.1	4096.51	7.79	4.03	0.008	759	1.0E-10	3.2E-13
	9				D	9.9	3984.58	6.40	3.95	0.006	641	9.9E-11	2.6E-13
	10				E	10.0	3832.76	8.65	3.99	0.009	900	9.9E-11	3.7E-13
	1	290		CM-II-1	A	7.6	2895.66	8.33	3.03	0.009	1146	7.5E-11	3.6E-13
	2				B	9.4	3847.73	5.49	3.76	0.005	570	9.4E-11	2.2E-13
	3				C	6.9	2756.45	7.21	2.75	0.007	1042	6.9E-11	3.0E-13
	4				D	6.5	2616.98	3.96	2.60	0.004	604	6.5E-11	1.6E-13
	5				E	6.0	2457.76	5.75	2.39	0.006	933	6.0E-11	2.3E-13
		293	28465 \pm 268										

* Stoichiometric calculations

& Nelson, 1991; Palacios-Fest, 1997; Palacios-Fest et al., 1993; Xia et al., 1997). Figure 4 shows Mg/Ca_v values at different parts of the lacustrine basin. Cano Magallanes mean values of Mg/Ca_v ranged from 0.0023–0.0036. Don Beto mean values fluctuated between 0.0026 and 0.0155, while El Diablo oscillated from 0.0015–0.0046. The Mg/Ca_v values from all three profiles are consistent in relation to each other (Table 4).

The Mg/Ca_v ratios from *Limnocythere ceriotuberosa* and *L. platyforma* generated estimated temperatures consistent with modern mean air winter (3.5 °C) and summer (20 °C) temperatures registered from San José Babicora, Las Varas and Gómez Farías for the time interval between 1971 and 1980 (Ortega-Ramírez et al., 1998). Mean water temperature estimates in Cano

Magallanes ranged from 6.5–7.9 \pm 0.4–1.2 °C. Don Beto mean water temperature estimates varied from 6.9–21.3 \pm 0.5–4.8 °C and El Diablo fluctuated between 5.6–9.1 \pm 0.2–1.7 °C (Table 4).

Interpretation

The Pleistocene-Holocene history

Interpretation of a lake's history requires the recognition of major hiatuses in any sequence and correlation among studied sites to determine periods of transgression and regression since gaps are not evident from the lithostratigraphy of the Babicora Basin but are indi-

cated in the paleoenvironmental reconstructions from ostracode trace elements. Two major zones, each divided into sub-zones, based on paleotemperature and paleosalinity, are shown in all three profiles. The lower zone (I) is divided into 4 sub-zones (Figure 4). Sub-zones 1 and 2 are bracketed between $28,465 \pm 268$ yrs B.P. and $16,342 \pm 200$ yrs B.P., and sub-zones 3 and 4 ranged from $16,342 \pm 200$ yrs B.P. and $10,976 \pm 115$ yrs B.P. The upper zone (II) is analyzed as a unit.

Zone I is well represented from Cano Magallanes, Don Beto and El Diablo profiles. Based upon radiocarbon dates obtained from Cano Magallanes ($28,465 \pm 268$ yrs B.P.), Don Beto ($24,470 \pm 765$ yrs B.P.) and El Diablo ($16,342 \pm 200$ yrs B.P.) we assume a relatively constant sedimentation rate at this interval (El Diablo, 0.012 cm yr^{-1} ; Don Beto, 0.007 cm yr^{-1} ; and Cano Magallanes, 0.006 cm yr^{-1}), thus, our results suggest that marine oxygen isotope Stage 2 (MOIS 2) is recorded by ostracode fauna and shell chemistry (Figures 3 & 4).

Dominance of *C. patzcuaro* associated with *L. platyforma* at the base of the record suggests an expanded cold water lake with fluctuating salinity. The trace element signals indicate that water temperature ranged from 5–10 °C. Salinity as suggested by faunal assemblages varied from oligo-haline to meso-haline during this episode at the shoreline and increased steadily toward the depocenter.

Sub-zone 1

Water inflow from the south (El Diablo) likely introduced a low-diversity assemblage, including *Limnocythere ceriotuberosa*, *L. bradburyi*, and *Candona patzcuaro* (Assemblage III). The two species of *Limnocythere* were dominant at this stage suggesting moderately saline conditions (Figure 4). The Mg/Ca_v ratios suggest low temperatures (5.6–9.1 °C). Toward the depocenter (Don Beto), the lake became gradually more saline (Assemblage III) while water temperature ranged between 7.6 and 9.9 °C. To the west (Cano Magallanes) faunal assemblages rapidly evolved from low salinity (Assemblage I) to moderate salinity (Assemblage III) at a relatively constant temperature (7.4–7.9°C), as well.

The low temperature values at El Diablo imply a seasonal cold water input probably from snowmelt. Increasing TDS through time suggests a reduction in effective humidity (after $28,465 \pm 268$ yrs B.P. and prior to $16,342 \pm 200$ yrs B.P.). The effective moisture reduction and the low temperatures after $28,465 \pm 268$ yrs B.P. and presumably before $\sim 18,000$ yrs B.P., sug-

gest a trend toward cool and dry conditions. Paleobotanical data from the northern Chihuahuan Desert in the Rio Grande village area (29° 13'N) at 610–680 m asl yielded juniper-grassland assemblages reflecting relatively drier climate (Van Devender, 1990). At higher elevations (from 880–1200 m asl) around the Big Bend area of Texas, a Piñon-juniper-oak assemblage is consistent with drier conditions (Van Devender, 1990). In Madrean Evergreen Woodland (between the Chihuahuan and Sonoran Deserts, where Laguna Babicora is located), mesophytic evergreen woodland communities characterized by sclerophyllous and microphyllous flora (Brown, 1994) predominated before, during and after the glacial maximum (22,000 to 17,000 yrs B.P.).

Sub-zone 2

Dilute water inflow (from the south: El Diablo) increased allowing a freshwater fauna (Assemblage I: *Candona patzcuaro*-dominated) to develop. The Mg/Ca_v ratios show a low temperature (6.6–7.4 °C). Toward the depocenter (Don Beto), faunal assemblages (II and III) reflect moderate salinity throughout most of the interval at a relatively constant temperature (~ 7 °C). The western shoreline area (Cano Magallanes) also shows a salinity decline from Assemblage II to I, while water temperature was similar to the other areas (6.6–7.2 °C).

During Sub-zone 2, atmospheric effective moisture increased as shown both by faunal assemblages and shell chemistry records. Lake level probably rose. The time break between Sub-zones 1 and 2 is marked by the collapse of Assemblage III and probably happened just before the glacial maximum ($24,470 \pm 765$ yrs B.P. to $16,342 \pm 200$ yrs B.P.). Decreasing salinity, as indicated by faunal assemblages suggest rising cold/wet conditions as a result of the equatorial migration of the main climatic belt.

Sub-zone 3

After a brief period of moderately saline water input, the southern source diluted again introducing the freshest water conditions recorded by ostracodes. The faunal assemblage present (Assemblage I) recorded in this sub-zone, are in good agreement with this interpretation. Water temperature also decreased to 6.1–6.5 °C, as suggested by Mg/Ca_v ratios. At this time the depocenter, characterized by Assemblage II, showed a slight decline in salinity as shown by the paleosalinity index, whereas water temperature increased to about 7.7–9.3 °C, as shown by Mg/Ca_v ratios.

Table 4. Temperature estimates derived from Mg/Ca, ratios of *Limnocythere* valves from: (a) El Diablo Profile, (b) Don Beto Profile and, (c) Cano Magallanes Profile. Temperature mean estimates include 2σ variability

Laguna Babiocra, Chihuahua			Jun-96								
Profile	Sequence #	Depth (cm)	Age (Years B.P.)	Sample #	Replicate	Valve Wt. (μ R)	m(Mg/Ca) (moles)		Temperature ($^{\circ}$ C)	Mean T	\pm
El Diablo	115	59	4346 \pm 105	ED-I-3	A	8.9	0.0041	0.0033	8.5	7.6	0.6
	116				B	13.7	0.0030		7.3		
	117				C	12.2	0.0032		7.5		
	118				D	15.5	0.0033		7.6		
	119				E	13.4	0.0028		7.0		
	120	72		ED-I-2	A	10.9	0.0023	0.0026	6.5	6.8	0.5
	121				B	14.0	0.0029		7.2		
	122				C	11.8	0.0027		7.0		
	123				D	14.8	0.0021		6.2		
	124				E	11.4	0.0030		7.3		
	125	92		ED-I-1	A	12.8	0.0035	0.0023	7.9	6.6	1.1
	126				B	9.2	0.0013		5.4		
	127				C	13.9	0.0014		5.5		
	128				D	11.2	0.0024		6.6		
	129				E	12.6	0.0031		7.5		
	130	100	10976 \pm 115	ED-II-3	A	14.0	0.0032	0.0027	7.6	7.0	0.5
	131				B	13.9	0.0028		7.1		
	132				C	14.0	0.0023		6.6		
	133				D	12.1	0.0021		6.3		
	134				E	13.0	0.0030		7.3		
	135	108		ED-II-2	A	14.0	0.0022	0.0028	6.5	7.0	0.4
	136				B	13.0	0.0030		7.3		
	137				C	11.5	0.0027		6.9		
	138				D	13.9	0.0033		7.6		
	139				E	10.5	0.0026		6.8		
	140	122		ED-II-1	A	12.3	0.0039	0.0027	8.4	7.0	0.8
	141				B	10.5	0.0026		6.8		
	142				C	10.8	0.0022		6.4		
	143				D	12.0	0.0025		6.7		
	144				E	12.4	0.0024		6.6		
	145	135		ED-III-3	A	15.5	0.0022	0.0020	6.4	6.1	0.2
	146				B	14.9	0.0019		6.1		
	147				C	15.0	0.0021		6.3		
	148				D	14.9	0.0016		5.8		
	149				E	26.4	0.0020		6.2		
	150	146		ED-III-2	A	12.9	0.0024	0.0020	6.6	6.1	0.4
	151				B	14.6	0.0017		5.8		
	152				C	15.0	0.0019		6.1		
	153				D	12.4	0.0015		5.7		
	154				E	14.8	0.0022		6.4		
155	154		ED-III-1	A	12.9	0.0027	0.0023	7.0	6.5	0.7	
156				B	14.9	0.0026		6.9			
157				C	14.4	0.0028		7.1			
158				D	15.7	0.0018		6.0			
159				E	12.8	0.0016		5.7			
160	166	16342 \pm 200	ED-IV-11	A	8.2	0.0022	0.0023	6.4	6.5	0.4	
161				B	9.9	0.0025		6.7			
162				C	8.3	0.0018		5.9			
163				D	10.7	0.0023		6.5			
164				E	8.7	0.0027		7.0			
165	176		ED-IV-10	A	11.5	0.0026	0.0031	6.8	7.4	0.7	
166				B	9.5	0.0024		6.7			
167				C	7.5	0.0030		7.3			
168				D	6.6	0.0037		8.0			
169				E	6.0	0.0038		8.2			
170	185		ED-IV-9	A	6.2	0.0024	0.0023	6.7	6.6	0.6	
171				B	12.8	0.0018		6.0			
172				C	7.6	0.0017		5.8			
173				D	7.8	0.0028		7.1			
174				E	8.3	0.0028		7.1			
175	192		ED-IV-8	A	9.8	0.0026	0.0025	6.8	6.8	1.2	
176				B	9.7	0.0020		6.2			
177				C	3.8	0.0044		8.9			
178				D	7.1	0.0016		5.7			
179				E	9.6	0.0022		6.4			
180	214		ED-IV-5	A	6.7	0.0028	0.0028	7.1	7.1	0.6	
181				B	9.9	0.0021		6.3			
182				C	7.2	0.0028		7.1			
183				D	7.7	0.0027		6.9			
184				E	4.7	0.0037		8.0			
185	219		ED-IV-4	A	7.0	0.0065	0.0046	11.2	9.1	1.7	
186				B	6.1	0.0032		7.5			
187				C	4.2	0.0052		9.8			
188				D	5.3	0.0050		9.6			
189				E	6.4	0.0029		7.2			
190	221		ED-IV-3	A	7.8	0.0020	0.0030	6.2	7.3	0.9	
191				B	7.2	0.0028		7.1			
192				C	4.0	0.0041		8.6			
193				D	8.9	0.0028		7.1			
194				E	5.2	0.0032		7.5			
195	228		ED-IV-2	A	8.4	0.0026	0.0016	6.8	5.7	0.6	
196				B	13.4	0.0015		5.6			
197				C	13.0	0.0014		5.5			
198				D	12.0	0.0013		5.4			
199				E	15.9	0.0011		5.2			
200	243		ED-IV-1	A	13.9	0.0013	0.0015	5.4	5.6	0.2	
201				B	13.0	0.0017		5.8			
202				C	13.1	0.0016		5.8			
203				D	14.7	0.0013		5.4			
204				E	11.6	0.0016		5.8			

Table 4. Continued

Profile	Sequence #	Depth (cm)	Age (Years B.P.)	Sample #	Replicate	Valve Wt. (μ g)	m(Mg/Ca) (moles)	(Mean)	Temperature ($^{\circ}$ C)	Mean T	\pm
Don Beto											
	111	35	1300 \pm 65	DB-I-5	A	6.9	0.0045	0.0038	9.0	8.2	0.9
	112				B	16.8	0.0035		7.8		
	113				C	15.8	0.0029		7.1		
	114				D	6.9	0.0042		8.7		
	106	71		DB-I-4	A	12.8	0.0119	0.0141	17.3	19.7	3.3
	107				B	14.2	0.0123		17.8		
	108				C	16.9	0.0182		24.4		
	109				D	22.1					
	110				E	22.6	0.0138		19.5		
	101	90		DB-I-3	A	22.1	0.0044	0.0098	8.9	15.0	3.8
	102				B	15.9	0.0113		16.6		
	103				C	25.5	0.0098		15.0		
	104				D	18.2	0.0101		15.3		
	105				E	15.1	0.0135		19.1		
	96	106		DB-I-2	A	13.3	0.0216	0.0155	28.2	21.3	4.8
	97				B	9.6	0.0173		23.3		
	98				C	12.8	0.0156		21.5		
	99				D	10.9	0.0108		16.0		
	100				E	12.1	0.0122		17.6		
	91	123		DB-I-1	A	14.0	0.0042	0.0047	8.6	9.2	2.0
	92				B	8.1					
	93				C	8.9					
	94				D	21.1	0.0033		7.6		
	95				E	8.3	0.0067		11.5		
	86	134		DB-II-9	A	10.0	0.0045	0.0049	9.0	9.4	1.8
	87				B	12.8	0.0049		9.4		
	88				C	9.3	0.0073		12.1		
	89				D	14.8	0.0027		7.0		
	90				E	9.1	0.0049		9.5		
	81	140	11885 \pm 315	DB-II-8	A	7.1	0.0057	0.0047	10.4	9.3	0.6
	82				B	11.4	0.0047		9.2		
	83				C	10.6	0.0042		8.7		
	84				D	9.3	0.0047		9.2		
	85				E	9.8	0.0045		8.9		
	76	152		DB-II-7	A	12.3	0.0028	0.0034	7.0	7.7	0.8
	77				B	9.9	0.0035		7.9		
	78				C	18.3	0.0045		9.0		
	79				D	11.8	0.0034		7.8		
	80				E	10.1	0.0027		7.0		
	71	165		DB-II-6	A	16.9	0.0024	0.0027	6.6	7.0	0.5
	72				B	14.8	0.0034		7.7		
	73				C	18.0	0.0022		6.4		
	74				D	16.0	0.0026		6.9		
	75				E	19.1	0.0030		7.3		
	66	176		DB-II-5	A	15.7	0.0031	0.0026	7.4	6.9	0.5
	67				B	21.3					
	68				C	12.8					
	69				D	17.2	0.0023		6.5		
	70				E	16.9	0.0025		6.7		
	61	190		DB-II-4	A	10.3	0.0051	0.0039	9.7	8.3	1.5
	62				B	21.3	0.0030		7.3		
	63				C	13.8	0.0043		8.8		
	64				D	21.1	0.0021		6.3		
	65				E	11.4	0.0049		9.5		
	56	200		DB-II-3	A	12.7	0.0043	0.0038	8.8	8.2	1.3
	57				B	14.7	0.0017		5.9		
	58				C	15.7	0.0039		8.4		
	59				D	10.0	0.0049		9.4		
	60				E	10.4	0.0041		8.6		
	51	218		DB-II-2	A	13.0	0.0033	0.0033	7.7	7.6	0.6
	52				B	11.9	0.0042		8.6		
	53				C	13.8	0.0030		7.3		
	54				D	10.4	0.0029		7.2		
	55				E	9.9	0.0030		7.3		
	46	230	24470 \pm 765	DB-II-1	A	8.2	0.0062	0.0053	10.9	9.9	1.4
	47				B	7.2	0.0061		10.8		
	48				C	10.0	0.0043		8.8		
	49				D	9.8	0.0036		8.0		
	50				E	5.7	0.0062		10.9		

Table 4. Continued

Profile	Sequence #	Depth (cm)	Age (Years B.P.)	Sample #	Replicate	Valve Wt. (μg)	m(Mg/Ca) (moles)		Temperature ($^{\circ}\text{C}$)	Mean T	\pm
Cano Magallanes											
		36	3503 \pm 101								
		78	7965 \pm 109								
		168	9614 \pm 130								
	41	220		CM-II-8	A	12.8	0.0025	0.0024	6.7	6.6	0.4
	42				B	12.9	0.0022		6.4		
	43				C	10.8	0.0020		6.2		
	44				D	11.0	0.0028		7.0		
	45				E						
	36	230		CM-II-7	A	17.0	0.0025	0.0023	6.8	6.5	0.6
	37				B	13.8	0.0032		7.6		
	38				C	15.8	0.0018		6.0		
	39				D	9.9	0.0022		6.4		
	40				E	4.8	0.0018		6.0		
	31	244		CM-II-6	A	8.9	0.0020	0.0024	6.2	6.6	0.7
	32				B	10.9	0.0024		6.6		
	33				C	10.9	0.0021		6.3		
	34				D	12.0	0.0020		6.1		
	35				E	8.1	0.0035		7.9		
	26	255		CM-II-5	A	10.4	0.0018	0.0029	6.0	7.2	0.8
	27				B	8.5	0.0031		7.4		
	28				C	5.1	0.0029		7.2		
	29				D	10.9	0.0028		7.1		
	30				E	6.2	0.0039		8.3		
	21	264		CM-II-4	A	7.0	0.0020	0.0023	6.1	6.6	0.5
	22				B	7.8	0.0022		6.4		
	23				C	8.0	0.0029		7.2		
	24				D	9.3	0.0020		6.1		
	25				E	9.6	0.0027		7.0		
	16	269		CM-II-3	A	8.0	0.0032	0.0035	7.5	7.9	0.4
	17				B	11.8					
	18				C	10.0					
	19				D	6.8	0.0038		8.2		
	20				E	6.8	0.0036		8.0		
	11	279		CM-II-2	A	10.9	0.0025	0.0031	6.8	7.5	1.1
	12				B	10.9	0.0033		7.6		
	13				C	10.8	0.0028		7.1		
	14				D	9.9	0.0023		6.5		
	15				E	6.1	0.0049		9.4		
	6	290			A	8.0	0.0018	0.0031	6.0	7.4	1.0
	7				B	7.4	0.0040		8.5		
	8				C	10.1	0.0031		7.5		
	9				D	9.9	0.0027		6.9		
	10				E	10.0	0.0037		8.1		
	1	290		CM-II-1	A	7.6	0.0047	0.0036	9.3	7.9	1.2
	2				B	9.4	0.0024		6.6		
	3				C	6.9	0.0043		8.8		
	4				D	6.5	0.0025		6.7		
	5			CM-II-1-1	E	6.0	0.0039		8.3		
		293	28,465 \pm 268								

To the west (Cano Magallanes), Laguna Babicora maintained a more diverse fauna that evolved from fresh-water (Assemblage I: *Candona patzcuaro*-dominated) to saline conditions (Assemblage III: *Limnocythere*-dominated) including the transitional Assemblage II (*Candona/Limnocythere* near equal proportions). Diversification requires relatively long-term water stability (no significant changes in salinity, temperature or water chemistry) favoring dilute conditions like those recorded by the paleosalinity index. Water temperature was almost

constant around 6.5 $^{\circ}\text{C}$ in this area as indicated by the Mg/Ca_v ratios.

The close temperature and paleosalinity index trends in the west and south suggests that the main source of water was from the south, although runoff may have occurred from other areas (i.e., western Cano Magallanes region). Effective moisture around the lake reached its maximum as suggested by the Cano Magallanes and Don Beto profiles. El Diablo received a large snowmelt inflow from the mountains (16,342 \pm

200 yrs B.P. to $11,885 \pm 315$ yrs B.P.). The coldest/wettest conditions prevailed in the lake at this time. Vigorous anti-cyclonic activity of the Mobile Polar Highs centers displaced the meteorologic equator south of the geographic equator (Leroux, 1993; Kutzbach et al., 1993), and the zonal westerlies were stronger in the troposphere (Williams, 1978; Harrison et al., 1984). Since there is no evidence of Pleistocene glaciers (McWilliams, personal communication, 1998) in the highlands of Babicora Basin to justify deglaciation water inflow, it is suggested that the region was strongly influenced by rainfall typical of temperate zones. Humid conditions are also reported from the northern part of the Chihuahuan Desert and in the Bolsón de Mapimi ($25^{\circ} 52'N$) where the playas supported pluvial lakes (Messing, 1986; Van Devender, 1990).

Sub-zone 4

Water inflow at El Diablo remained dilute, supporting Assemblage I and occasionally Assemblage II fauna while temperature remained stable ($\sim 7^{\circ}C$) as shown by Mg/Ca_v ratios. Toward the depocenter salinity rapidly rose and ostracode Assemblage I was replaced by Assemblage III as mean temperature reached $\sim 9.4^{\circ}C$ (as inferred from Mg/Ca_v ratios). To the west (Cano Magallanes) interpretation of the monospecific faunal Assemblage I and salinity index shows a decline to its lowest level while the Mg/Ca_v ratios indicate relatively constant temperature ($\sim 6.5^{\circ}C$) recorded across the basin.

Although dilute water input continued from the south, the western area contributed significant volumes during snowmelt events. A period of relatively decreasing effective moisture characterized the end of the Pleistocene as a result of increasing solar radiation (Kutzbach & Wright, 1985; Spaulding & Graumlich, 1986; COHMAP, 1989; Spaulding, 1990, 1991) which contributed to the retreat of the Laurentide Ice Sheet.

Zone II covers the period from the end of the Pleistocene to the late Holocene. Based upon ostracode shell chemistry this zone was characterized by fluctuating conditions. During the late Pleistocene and early Holocene ($\sim 11,000$ yrs B.P.) the lake shrank considerably. However, short and intense runoff episodes are recorded by ostracode diversity and abundance in El Diablo and Don Beto profiles and by sedimentologic features of the lacustrine and bog deposits of Cano Magallanes profile (Ortega-Ramírez et al., 1998). With decreasing lake-level, the western area became paludal whereas the southern portion accumulated lacustrine and water-laid deposits. At El Diablo, faunal

assemblages (I and II) along with salinity index values suggest dilute water input, whereas at Don Beto evidence of salinization is shown by the salinity index. Low temperature estimates ($6.6\text{--}7.6^{\circ}C$) are controversial and difficult to explain because they are in contrast with the Don Beto profile where Mg/Ca_v ratios increase at this time suggesting temperatures between 8.2 and $21.3^{\circ}C$.

During the middle Holocene (8,900 to 4,000 yrs B.P.), effective humidity decreased significantly as water temperature fluctuated in Laguna Babicora. A warm interval was recorded by Mg/Ca_v ; water temperature reached $21.3^{\circ}C$. Bog and eolian deposits that accumulated during this time support this interpretation (Ortega-Ramírez et al., 1998). In addition, warm/dry conditions for this time interval are reported elsewhere in the Southwest (Markgraf et al., 1984; Spaulding & Graumlich, 1986; Oviatt, 1988). Net moisture deficit is also interpreted by a decrease in magnetic minerals (Urrutia-Fucugauchi et al., 1997), increased calcium carbonate concretions (Metcalfe et al., 1997), and loess-like deposits (Ortega-Ramírez et al., 1998).

During the late Holocene ($\sim 4,000$ yrs B.P.), ostracode shell chemistry shows a sharp temperature decline to $\sim 8.2^{\circ}C$ based on Mg/Ca_v ratios. Increased effective moisture at low temperature probably resulted from cold winters around the lake (between $4,346 \pm 105$ yrs B.P. and $1,300 \pm 65$ yrs B.P.). Short-term climatic anomalies in Laguna Babicora have been inferred by wetland deposits, paleosols, flood deposits and erosional surfaces (Ortega-Ramírez, 1990, 1995). At this last period, the seasonal insolation anomalies in both hemispheres declined (Street-Perrot, 1993), weakening the pressure and circulation in the northern hemisphere.

Discussion

Environmental estimates derived from the trace element chemistry of *Limnocythere* spp. are compared with modern parameters recorded in the locality to determine feasibility. Temperature estimates are consistent, as established in an earlier section, with the modern winter and summer mean air temperatures suggesting that experimental standards used in this study generate numbers fitting within natural ranges.

The ostracode species present at Laguna Babicora reach maturity between 4–12 weeks (Forester, personal communication, 1989). Because of its short life cycle, the genus *Limnocythere* may produce more than one generation within a year, thus seasonal variation may be

observed in the shell chemistry record. The implication of this correlation is that water temperature at the time the lake was active ranged between 3 and 22 °C.

To assume a water/atmosphere temperature correlation would imply that Laguna Babicora was a shallow lake. In contrast to Metcalfe et al. (1997), we argue that Laguna Babicora was not a deep lake. The occurrence of *Stephanodiscus niagarae* (a planktonic, deepwater diatom) may also respond to cold, freshwater input and not necessarily to water depth, since it is a winter-blooming species (Conley et al., 1993). The diatom benthic/planktonic ratio suggests that when planktonic forms dominate, high lake stages occur (e.g., Lago de Pátzcuaro, Bradbury, 1988). This is not contrary to our findings: part of ZI-3 correlates with the high stand in the full glacial reported by Metcalfe et al. (1997) where planktonic diatoms overrate benthic diatoms. Thompson et al. (1993) suggested that flat-floored, shallow lakes are relatively insensitive to late-Quaternary climatic variations. Ortega-Ramírez (1995a) defined Babicora Basin as a graben, thus the depocenter readily formed a flat-floored surface. Ortega-Ramírez et al. (1998) demonstrated the occurrence of post-depositional dissolution voids in massive sediments in the basin that formed during shallow-perennial-lake conditions during the early Holocene. In addition, geomorphic evidence indicates that Laguna Babicora underwent horizontal variations in response to long periods of precipitation, hence forming an expanded-shallow-lake (Ortega-Ramírez, 1990, 1995a). Limited faunal and shell chemistry variations at the time of maximum lake level conditions are consistent with a shallow lake.

A salinity gradient from shoreline to the depocenter gradually increases in endorreic basins as shown in Laguna Babicora. Temperature gradients are similar between Don Beto and Cano Magallanes but lower at the effluent area (El Diablo), because of its geomorphological setting.

Based upon ostracode paleoecology and shell chemistry we infer that Laguna Babicora was a monomictic lake open to circulation for a short time during late spring to early fall. During MOIS 2, snowmelt water input induced surface and deep water mixing. The lake remained well mixed for about four months annually providing time for *Candona caudata* and *C. patzcuaro* to complete their life cycle. The rest of the year the lake either had an ice cover or was too cold to permit ostracodes hatching and molting. Shell chemistry-derived temperatures are in good agreement with modern temperate monomictic lakes where maximum water tem-

perature reaches about 8 °C (Cole, 1979; Margalef, 1983). However, to test this interpretation trace elements from ostracode valves from these types of lakes will be required.

Age control of all three profiles indicates that Laguna Babicora was a permanent lake throughout the late Pleistocene but it became intermittent during the Holocene, with only the depocenter (Don Beto) remaining as a smaller water body. Urrutia-Fucugauchi et al. (1997) interpreted the western profile (Cano Magallanes) as old as 11,000 yrs B.P. based on a ¹⁴C date of 9,614 ± 130 yrs B.P. recorded at a depth of 168 cm; but a recently obtained date near the base of the profile, provided an age of 28,465 ± 268 yrs B.P. at a depth of 279 cm and demonstrates that the western area was under water at a much earlier date. Correlation between this date and that at the base of profile Don Beto (24,470 ± 765 yrs B.P.) confirms our interpretation.

In summary, based on ostracode shell chemistry, we find two major paleoclimatic zones (I and II), characterized by fluctuating conditions. Paleoenvironmental zone ZI-1 pre-dates the glacial maximum and marks a period of prevalent cold/dry conditions. ZI-2 records the beginning of the full glacial and represents cold/wet conditions. ZI-3 represents the maximum lake extension with the coldest/wettest characteristics. ZI-4 shows environmental change to dryer conditions. At the beginning of the early Holocene (probably during the Younger Dryas), El Diablo supported Assemblage I while Cano Magallanes evolved into a bog system with salinity tolerant species (*L. bradburyi*) and, Don Beto was the only area continuously inundated permitting the development of Assemblage III ostracodes to persist as salinity rose.

Shell chemistry data are consistent with the interpretations of Urrutia-Fucugauchi et al. (1997), Metcalfe et al. (1997) and Ortega-Ramírez et al. (1999) who recognized a general trend of increasing dryness and warmer temperatures in the region. More detailed and uniform sampling strategies will help improve our knowledge of Laguna Babicora.

Acknowledgements

Financial support for the data acquisition was provided through grants from National Council of Science and Technology (CONACyT 3732-T9302) and National University of Mexico (DGAPA IN104494). Shell chemistry analysis was conducted in the Laboratory of Trace Elements and Stable Isotopes of the University

of Arizona. The critical comments and suggestions by Peter Swarzensky, from the USGS (St. Petersburg, Florida) and Art McWilliams from the University of Arizona are greatly appreciated. Our unknown reviewers raised invaluable questions and issues that we attempted to answer with the best of our knowledge.

References

- Berger, A., T. Fichefet, H. Galle, I. Marsiat, C. Tricot & P. van Ypersele, 1990. Ice sheet and sea level change as a response to climatic change at the astronomical time scale. In Paepe, R. (ed.), *Greenhouse Effect, Sea Level and Drought*. Kluwer Publishers, 85–107.
- Bradbury, J. P., 1988. A paleolimnological record of climate from Lago de Pátzcuaro for the past 45 Ky. Northern Hemisphere-Southern Hemisphere Interconnections. 15th Biennial Meeting of the American Quaternary Association, 5–7 September, Puerto Vallarta, Mexico. UNAM-UMEC, p. 91. (Program and abstracts).
- Brisson, R. A. & W. P. Lowry, 1955. Synoptic climatology of the Arizona summer precipitation singularity. *Bull. Am. Meteorol. Soc.* 36: 329–339.
- Brown, D. E., 1994. Madrean Evergreen Woodland; Section 123.3, Part 2. In Brown, D. E. (ed.), *Biotic Communities – Southwestern United States and Northwestern Mexico*. University of Utah Press, Salt Lake City, 59–65.
- Chivas, A. R., P. De Deckker & J. M. G. Shelley, 1983. Magnesium, strontium and barium partitioning in nonmarine ostracod shells and their use in paleoenvironmental reconstructions: A preliminary study. In Maddocks, R. F. (ed.), *Applications of Ostracoda*. University of Houston, Houston, Geosciences, 238–249.
- Chivas, A. R., P. De Deckker & J. M. G. Shelley, 1986a. Magnesium and strontium in nonmarine ostracod shells: A new paleosalinometer and paleothermometer. *Palaeogeogr. Palaeoclimatol. Palaeoecol.* 54: 43–61.
- Chivas, A. R., P. De Deckker & J. M. G. Shelley, 1986b. Magnesium and strontium in nonmarine ostracod shells as indicators of paleosalinity and paleotemperature. *Hydrobiologia* 143: 135–142.
- Chivas, A. R., P. De Deckker, J. A. Cali, E. Kiss & J. M. G. Shelley, 1993. Coupled stable-isotope and trace-element measurements of lacustrine carbonates as paleoclimatic indicators. In Swart, P. K., K. C. Lohman, J. McKenzie & S. Savin (eds), *Climate Change in Continental Isotopic Records*. Geophysical Monograph 78. Washington, D.C.: American Geophysical Union, 113–121.
- CLIMAP Project Members, 1981. Seasonal reconstruction of the earth's surface at the last glacial maximum. *Geological Society of America, Map and Chart Series MC-36*.
- Cohen, A. S., M. R. Palacios-Fest, R. M. Negrini, P. E. Wigand & D. Erbes, 2000. High resolution continental paleoclimate record for the middle-late Pleistocene from Summer Lake, Oregon, USA: II: Evidence of paleoenvironmental change from sedimentology, paleontology and geochemistry. *J. Paleolim.* 24: 151–182.
- COHMAP Members, 1988. Climatic changes of the last 18,000 years: Observations and model simulations. *Science* 191: 1131–1137.
- COHMAP Members, 1989. Major climatic changes of the last 18,000 years: Observations and model simulations. *Science* 241: 1043–1052.
- Cole, G. A., 1979. *Textbook of Limnology*. 2nd ed. The C. V. Mosby Company, St. Louis, 426 pp.
- Conley, D. J., C. L. Schelske & E. F. Stoermer, 1993. Modification of the biogeochemical cycle of silica with eutrophication. *Marine Ecol. Prog. Ser.* 101: 179–192.
- Delorme, L. D., 1969. Ostracodes as Quaternary paleoecological indicators. *Can. J. Earth Sci.* 6: 1471–1475.
- Delorme, L. D., 1989. Methods in Quaternary ecology. 7: Freshwater ostracodes. *Geosci. Can.* 16: 85–90.
- Elias, S. A. & T. R. Van Devender, 1990. Fossil insect evidence for late Quaternary climatic change in the Big Bend region, Chihuahuan Desert, Texas. *Quat. Res.* 34: 249–261.
- Engstrom, D. & S. Nelson, 1991. Paleosalinity from trace metals in fossil ostracodes compared with observational records at Devils Lake, North Dakota, USA. *Palaeogeogr. Palaeoclimatol. Palaeoecol.* 83: 295–312.
- Enzel, Y., L. Ely, B. Allen & M. R. Palacios-Fest, (in prep). Paleo-environmental reconstruction of lacustrine systems of Northern Baja California, Mexico. (Research funded by the National Geographic Society).
- Eugster, H. P. & L. A. Hardie, 1978. Saline lakes, Chapter 8. In Lerman, A. (ed.), *Lakes: Chemistry, Geology, Physics*. Springer-Verlag, Berlin, 237–294.
- Forester, R. M., 1983. Relationship of two lacustrine ostracode species to solute composition and salinity: implications for paleohydrochemistry. *Geology* 11: 435–438.
- Forester, R. M., 1987. Late Quaternary paleoclimate records from lacustrine ostracodes. In Ruddiman, W. F. & H. E. Wright (eds), *North America and Adjacent Oceans During the Last Deglaciation*. The Geology of North America, vol. K-3. Geological Society of America, Boulder, Colorado, 261–276.
- Forester, R. M., 1991. Ostracode assemblages from springs in the western United States: implications for paleohydrology. *Mem. ent. Soc. Can.* 155: 181–201.
- García, E., 1973. Modificaciones al sistema de clasificación climática de Köppen (para adaptarlo a las condiciones de la República Mexicana). *Bol. Inst. de Geogr., UNAM, Mexico, D.F.*, 246 pp.
- Hales, J. R. E. Jr., 1974. South-western United States summer monsoon source – Gulf of Mexico or Pacific Ocean. *J. Appl. Meteorol.* 13: 331–342.
- Harrison, S. P., S. E. Metcalfe, A. B. Pittock, C. N. Roberts, M. J. Salinger & F. A. Street-Perrot, 1984. A climatic model of the last glacial/interglacial transition based on paleotemperature and paleohydrological evidence. In Vogel, J. C. (ed.), *Late Cainozoic Paleoclimates of the Southern Hemisphere*. A. A. Balkema, Rotterdam, 21–34.
- Instituto Nacional de Estadística, Geografía e Informática (INEGI), 1990. Estudio hidrológico de la Alta Babicora, Chihuahua, anexo cartas. INEGI, Mexico, D.F., 143 pp.
- Irwin-Williams, C. & C. V. Haynes, 1970. Climatic change and early population dynamics in the southwestern United States. *Quat. Res.* 1: 59–71.
- Kutzbach, J. E., P. J. Guetter, P. J. Behling & R. Selen, 1993. Simulated climatic changes. Results of the COHMAP climate-model experiments. In Wright, H. E. Jr., J. E. Kutzbach, T. Webb III, W. F. Ruddiman, F. A. Street-Perrot & P. J. Bartlein (eds). *Global Climates Since the Last Glacial Maximum*. University of Minnesota Press, Minneapolis, 24–93.

- Kutzbach, J. E. & H. E. Wright Jr., 1985. Simulation of the climate of 18,000 years B.P.: Results for the North American/North Atlantic/European sector and comparison with the geologic record of North America. *Quat. Sci. Rev.* 4: 147–187.
- Leroux, M., 1993. The Mobile Polar High: A new concept explaining present mechanisms of meridional air-mass and energy exchanges and global propagation of paleoclimatic changes. *Global and Planetary Change* 7: 69–93.
- Margalef, R., 1983. *Limnología*. Ediciones Omega, S.A., Barcelona, 1010 pp.
- Markgraf, V., J. P. Bradbury, R. M. Forester, G. Singh & R. S. Strenberg, 1984. San Agustin Plains, New Mexico: Age and paleoenvironmental potential reassessed. *Quat. Res.* 22: 336–343.
- Messing, H. J., 1986. A late Pleistocene-Holocene fauna from Chihuahua, Mexico. *The Southwestern Naturalist* 31: 277–288.
- Metcalfé, S. E., A. Bimpson, A. J. Courtice, S. L. O'Hara & D. M. Taylor, 1997. Climate change at the monsoon westerly boundary in northern Mexico. *J. Paleolim.* 17: 155–171.
- Meyer, E. R., 1973. Late Quaternary paleoecology of the Cuatro Ciénegas Basin, Coahuila, Mexico. *Ecology* 54: 982–995.
- Nelson, R. P., 1986. High-resolution climatic analysis and Southwest biogeography. *Science* 232: 27–34.
- Ortega-Ramírez, J., 1990. Le sommet du remplissage Quaternaire de la Laguna Babicora (Etat de Chihuahua, Nord-Ouest du Mexique): reconstruction des paléoenvironnements à partir de la sédimentologie et de la stratigraphie. Thèse de Doctorat de l'Université Louis Pasteur de Strasbourg, France, 345 pp.
- Ortega-Ramírez, J., 1995a. Los paleoambientes holocénicos de la Laguna Babicora, Chihuahua, México. *Geofis. Int.* 34: 107–116.
- Ortega-Ramírez, J., 1995b. Correlación estratigráfica de los depósitos cuaternarios de la Laguna Babicora, Chihuahua, México. *Geofis. Int.* 34: 117–129.
- Ortega-Ramírez, J., A. Valiente-Banuet, J. Urrutia-Fucugauchi, C. A. Mortera-Gutiérrez & G. Alvarado-Valdéz, 1998. Paleoclimatic changes during the late Pleistocene-Holocene in Laguna Babicora, Chihuahuan Desert, Mexico. *Can. J. Earth Sci.* 35: 1168–1179.
- Oviatt, C. G., 1988. Late Pleistocene and Holocene lake fluctuations in the Sevier Lake Basin, Utah, USA. *J. Paleolim.* 1: 9–21.
- Palacios-Fest, M. R., 1996. Geoquímica de la concha de ostrácodos (*Limnocythere staplini*): Un método de regresión múltiple como indicador paleoclimático. *GEOS* 16: 130–136.
- Palacios-Fest, M. R., 1997. Paleoenvironmental reconstruction of human activity in Central Arizona using shell chemistry of Hohokam canal ostracodes. *Geoarchaeology* 12: 211–226.
- Palacios-Fest, M. R. & D. L. Dettman, in press. Temperature controls monthly variation in ostracode valve Mg/Ca: *Cypridopsis vidua* from a small lake in Sonora, Mexico. *Geochim. Cosmochim. Acta*.
- Palacios-Fest, M. R., A. S. Cohen, J. Ruiz & B. Blank, 1993. Comparative paleoclimatic interpretations from nonmarine ostracodes using faunal assemblages, trace elements shell chemistry and stable isotope data. In Swart, P., J. McKenzie & K. C. Lohman (eds), *Climate Change in Continental Isotopic Records*. American Geophysical Union, Washington, D.C., *Geophysical Monograph* 78, 179–190.
- Phelp, A. L., 1990. A Clovis projectile point from the vicinity of Samalayuca, Chihuahua, Mexico. *The Artifact* 28: 49–51.
- Powell, A. M. & R. A. Hilsenbeck, 1995. An introduction to the Chihuahuan Desert region, part II: Flora. *Chihuahuan Desert Discovery Magazine of the Chihuahuan Desert Research Institute* 35: 4–14.
- Ruddiman, W. F. & J. C. Duplessy, 1985. Conference of the last deglaciation: Timing and mechanisms. *Quat. Res.* 23: 1–17.
- Spaulding, W. G., 1990. Vegetational and climatic development of the Mojave Desert: The last glacial maximum to the present. In Betancourt, J. L., T. Van Devender & P. Martin (eds), *Packrat Middens: The Last 40,000 years of Biotic Change*. The University of Arizona Press, Tucson, 167–199.
- Spaulding, W. G., 1991. Pluvial climatic episodes in North America and North Africa: Types and correlation with global climate. *Palaeogeogr. Palaeoclimatol. Palaeoecol.* 84: 217–227.
- Spaulding, W. G. & L. J. Graumlich, 1986. The last pluvial climatic episodes in the deserts of southwestern North America. *Nature* 230: 441–444.
- Street-Perrot, F. A. & Perrot, R. A., 1993. Holocene vegetation, lake levels, and climate of Africa. In Wright, H. E. Jr., J. E. Kutzbach, T. Webb III, W. F. Ruddiman, F. A. Street-Perrot & P. J. Bartlein (eds), *Global Climate Since the Last Glacial Maximum*. University of Minnesota Press, 318–356.
- Thompson, R. S., C. Whitlock, P. J. Bartlein, S. P. Harrison & W. G. Spaulding, 1993. Climatic changes in the western United States since 18,000 yr B.P. In Wright, H. E. Jr., J. E. Kutzbach, T. Webb III, W. F. Ruddiman, F. A. Street-Perrot & P. J. Bartlein (eds), *Global Climate Since the Last Glacial Maximum*. University of Minnesota Press, 468–513.
- Tomney, R. S. III, M. D. Blum & S. Valastro Jr., 1993. Late Quaternary climates and environments of Edwards Plateau, Texas. *Global and Planetary Change* 7: 299–320.
- Urrutia-Fucugauchi, J., J. Ortega-Ramírez & R. Cruz-García, 1997. Rock-magnetic study of late Pleistocene-Holocene sediments from the Babicora lacustrine basin, Chihuahua, northern Mexico. *Geofis. Int.* 36: 77–86.
- Van Devender, T. R., 1977. Holocene woodlands in the Southwestern Desert. *Science* 198: 189–192.
- Van Devender, T. R., 1990. Late Quaternary vegetation and climate of the Chihuahuan Desert, United States and Mexico. In Betancourt, J. L., T. Van Devender & P. Martin (eds), *Packrat Middens: The Last 40,000 Years of Biotic Change*. The University of Arizona Press, Tucson, 105–133.
- Van Devender, T. R. & T. L. Burgess, 1985. Late Pleistocene woodlands in the Bolsón de Mapimi: A refugium for the Chihuahuan Desert biota? *Quat. Res.* 24: 346–353.
- Van Devender, T. R. & W. G. Spaulding, 1979. Development of vegetation and climate in the southern United States. *Science* 204: 701–710.
- Van Devender, T. R., R. S. Thompson & J. L. Betancourt, 1987. Vegetation history of the deserts of the southwest of North America: The nature and timing of the late Wisconsin-Holocene transition. In Ruddiman, W. F. & H. E. Wright Jr. (eds), *North America and Adjacent Oceans During the Last Deglaciation*. *The Geology of North America*, vol. K-3. Geological Society of America, Boulder, Colorado, 323–352.
- Wansard, G., 1996. Quantification of paleotemperature changes during isotopic stage 2 in the La Draga continental sequence (NE Spain) based on the Mg/Ca ratio of freshwater ostracods. *Quat. Sci. Rev.* 15: 237–245.
- Waters, M., 1989. Late Quaternary lacustrine history and paleoclimatic significance of pluvial Lake Cochise, Southeastern Arizona. *Quat. Res.* 32: 1–11.

- Wells, P. V., 1966. Late Pleistocene and degree of pluvial climate change in the Chihuahuan Desert. *Science* 16: 970–975.
- Williams, J., 1978. A brief comparison of model simulations of glacial period maximum atmospheric circulation. *Palaeogeogr. Palaeoclimatol. Palaeoecol.* 25: 191–198.

- Xia, J., E. Ito & D. R. Engstrom, 1997. Geochemistry of ostracode calcite: Part I. An experimental determination of oxygen isotope fractionation. *Geochim. Cosmochim. Acta* 61: 377–382.